Digital Change Detection

12

Biophysical materials and human-made features on the surface of Earth are inventoried using remote sensing and *in situ* techniques. Some of the data are fairly static; they do not change over time. Conversely, some biophysical materials and human-made features are dynamic, changing rapidly. It is important that such changes be inventoried accurately so that the physical and human processes at work can be more fully understood (Lunetta and Elvidge, 2000; Zhan et al., 2002). In fact, it is believed that land-use/land-cover change is a major component of global change with an impact perhaps greater than that of climate change (Skole, 1994; Foody, 2001). It is not surprising, therefore, that significant effort has gone into the development of change detection methods using remotely sensed data (e.g., Jensen et al., 1997; Maas, 1999; Song et al., 2001; Arzandeh and Wang, 2003; Lunetta and Lyons, 2003). This chapter reviews how change information is extracted from digital remotely sensed data. It summarizes the remote sensor system and environmental parameters that must be considered when change detection takes place. Several of the most widely used change detection algorithms are introduced and demonstrated.

Steps Required to Perform Change Detection

The general steps required to perform digital change detection using remotely sensed data are summarized in Figure 12-1.

Change Detection Geographic Region of Interest

The dimensions of the change detection region of interest (ROI) must be carefully identified and held constant throughout a change detection project. The geographic ROI (e.g., a county, state, or watershed) is especially important in a change detection study because it must be completely covered by *n* dates of imagery. Failure to ensure that each of the multiple-date images covers the geographic area of interest results in change detection maps with data voids that are problematic when computing change statistics.

Change Detection Time Period

Sometimes change detection studies are overly ambitious in their attempt to monitor changes in the landscape. Sometimes the time period selected over

which change is to be monitored is too short or too long to capture the information of interest. Therefore, the analyst must be careful to identify the optimal change detection time period(s). This selection, of course, is dictated by the nature of the problem. Traffic transportation studies might require a change detection period of just a few seconds or minutes. Conversely, images obtained monthly or seasonally might be sufficient to monitor the greening of a continent. Careful selection of the change detection time period can ensure that resource analysis funds are not wasted.

Select an Appropriate Land-use/Land-cover Classification System

As discussed in Chapter 9, it is wise to use an established, standardized land-cover/land-use classification system for change detection, such as the following:

- American Planning Association *Land-Based Classification Standard* (LBCS),
- U.S. Geological Survey *Land Use/Land Cover Classification System for Use with Remote Sensor Data*,
- U.S. *National Vegetation Classification System* (NVCS),
- U.S. Fish and Wildlife Service *Classification of Wetlands and Deepwater Habitats of the United States*, and
- International Geosphere-Biosphere Program *Land Cover Classification System*.

The use of standardized classification systems allows change information to be compared with other studies.

Hard and Fuzzy Change Detection Logic

Most change detection studies have been based on the comparison of multiple-date *hard* land-cover classifications of remotely sensed data. The result is the creation of a *hard* change detection map consisting of information about the change in discrete categories (e.g., change in forest, agriculture). This is still very important and practical in many instances, but we now recognize that it is ideal to capture both discrete and fuzzy changes in the landscape (refer to Chapter 9 for a discussion about fuzzy land-cover classification).

Land-cover changes may range from no landscape alteration whatsoever, through modifications of variable intensity, to a full transformation or conversion to an entirely new class (e.g., the Denver, CO, example later in this chapter). Scientists now believe that replacing the Date n and Date $n + 1$ hard classification maps typically used in a change detection project with fuzzy classification maps will result in more informative and accurate land-cover change information (Foody, 2001; Woodcock et al., 2001).

Per-pixel or Object-oriented Change Detection

The majority of digital image change detection has been based on processing Date n and Date $n + 1$ classification maps pixel by pixel. This is commonly referred to as *per pixel* change detection. *Object-oriented* change detection involves the comparison of two or more scenes consisting of many relatively homogenous image objects (patches or segments) that were identified using the techniques discussed in Chapter 9. The smaller number of relatively homogeneous image objects in the two scenes are then subjected to change detection techniques discussed in this chapter.

Remote Sensing System Considerations

Successful remote sensing change detection requires careful attention to:

- remote sensor system considerations, and
- environmental characteristics.

Failure to understand the impact of the various parameters on the change detection process can lead to inaccurate results (Dobson et al., 1995; Yuan and Elvidge, 1998). Ideally, the remotely sensed data used to perform change detection is acquired by a remote sensor system that holds the following resolutions constant: temporal, spatial (and look angle), spectral, and radiometric. It is instructive to review each of these parameters and identify why they can have a significant impact on the success of a remote sensing change detection project.

Temporal Resolution

Two important temporal resolutions should be held constant during change detection using multiple dates of remotely sensed data. First, the data should be obtained from a sensor system that acquires data at approximately the *same time of day*. For example, Landsat Thematic Mapper data are acquired before 9:45 a.m. for most of the conterminous United States. This eliminates diurnal Sun angle effects that

which change is to be monitored is too short or too long to capture the information of interest. Therefore, the analyst must be careful to identify the optimal change detection time period(s). This selection, of course, is dictated by the nature of the problem. Traffic transportation studies might require a change detection period of just a few seconds or minutes. Conversely, images obtained monthly or seasonally might be sufficient to monitor the greening of a continent. Careful selection of the change detection time period can ensure that resource analysis funds are not wasted.

Select an Appropriate Land-use/Land-cover Classification System

As discussed in Chapter 9, it is wise to use an established, standardized land-cover/land-use classification system for change detection, such as the following:

- American Planning Association *Land-Based Classification Standard* (LBCS),
- U.S. Geological Survey *Land Use/Land Cover Classification System for Use with Remote Sensor Data*,
- U.S. *National Vegetation Classification System* (NVCS),
- U.S. Fish and Wildlife Service *Classification of Wetlands and Deepwater Habitats of the United States*, and
- International Geosphere-Biosphere Program *Land Cover Classification System*.

The use of standardized classification systems allows change information to be compared with other studies.

Hard and Fuzzy Change Detection Logic

Most change detection studies have been based on the comparison of multiple-date *hard* land-cover classifications of remotely sensed data. The result is the creation of a *hard* change detection map consisting of information about the change in discrete categories (e.g., change in forest, agriculture). This is still very important and practical in many instances, but we now recognize that it is ideal to capture both discrete and fuzzy changes in the landscape (refer to Chapter 9 for a discussion about fuzzy land-cover classification).

Land-cover changes may range from no landscape alteration whatsoever, through modifications of variable intensity, to a full transformation or conversion to an entirely new class (e.g., the Denver, CO, example later in this chapter). Scientists now believe that replacing the Date n and Date $n + 1$ hard classification maps typically used in a change detection project with fuzzy classification maps will result in more informative and accurate land-cover change information (Foody, 2001; Woodcock et al., 2001).

Per-pixel or Object-oriented Change Detection

The majority of digital image change detection has been based on processing Date n and Date $n + 1$ classification maps pixel by pixel. This is commonly referred to as *per pixel* change detection. *Object-oriented* change detection involves the comparison of two or more scenes consisting of many relatively homogenous image objects (patches or segments) that were identified using the techniques discussed in Chapter 9. The smaller number of relatively homogeneous image objects in the two scenes are then subjected to change detection techniques discussed in this chapter.

Remote Sensing System Considerations

Successful remote sensing change detection requires careful attention to:

- remote sensor system considerations, and
- environmental characteristics.

Failure to understand the impact of the various parameters on the change detection process can lead to inaccurate results (Dobson et al., 1995; Yuan and Elvidge, 1998). Ideally, the remotely sensed data used to perform change detection is acquired by a remote sensor system that holds the following resolutions constant: temporal, spatial (and look angle), spectral, and radiometric. It is instructive to review each of these parameters and identify why they can have a significant impact on the success of a remote sensing change detection project.

Temporal Resolution

Two important temporal resolutions should be held constant during change detection using multiple dates of remotely sensed data. First, the data should be obtained from a sensor system that acquires data at approximately the *same time of day*. For example, Landsat Thematic Mapper data are acquired before 9:45 a.m. for most of the conterminous United States. This eliminates diurnal Sun angle effects that

General Steps Used to Conduct Digital Change Detection Using Remote Sensor Data

State the nature of the change detection problem.
- * Specify change detection geographic region of interest.
- * Specify change detection time period (e.g., daily, seasonal, yearly).
- * Define the classes of interest in a classification system.
- * Select hard and/or fuzzy change detection logic.
- * Select per-pixel or object-oriented change detection.

Considerations of significance when performing change detection.
- * Remote sensing system considerations:
  - Spatial, spectral, temporal, and radiometric resolution
- * Environmental considerations:
  - Atmospheric conditions
  - Soil moisture conditions
  - Phenological cycle characteristics
  - Tidal stage, etc.

Process remote sensor data to extract change information.
- * Acquire appropriate change detection data:
  - *In situ* and collateral data
  - Remotely sensed data:
    - Base year (time n)
    - Subsequent year(s) (time n - 1 or n + 1)
- * Preprocess the multiple-date remote sensor data:
  - Geometric correction
  - Radiometric correction (or normalization)
- * Select change detection algorithm.
- * Apply appropriate image classification logic if necessary:
  - Supervised, unsupervised, hybrid
- * Perform change detection using GIS algorithms:
  - Highlight selected classes using change detection matrix
  - Generate change-map products
  - Compute change statistics

Perform accuracy assessment.
- * Select method:
  - Qualitative confidence building
  - Statistical measurement
- * Determine number of samples required by class.
- * Select sampling scheme.
- * Obtain ground reference test information.
- * Create and analyze change detection error matrix:
  - Univariate and multivariate statistical analysis

Accept or reject previously stated hypothesis.
Distribute results if accuracy is acceptable.

Figure 12-1 The general steps used to perform digital change detection of remotely sensed data.

CHAPTER 12 Digital Change Detection

can cause anomalous differences in the reflectance properties of the remotely sensed data. Second, whenever possible it is desirable to use remotely sensed data acquired on *anniversary dates*, for example, February 1, 2004, and February 1, 2005. Using anniversary date imagery minimizes the influence of seasonal Sun-angle and plant phenological differences that can negatively impact a change detection project (Jensen et al., 1993a).

Spatial Resolution and Look Angle

Accurate spatial registration of at least two images is essential for digital change detection. Ideally, the remotely sensed data are acquired by a sensor system that collects data with the same *instantaneous field of view* on each date. For example, Landsat Thematic Mapper data collected at 30×30 m spatial resolution on two dates are relatively easy to register to one another. It is possible to perform change detection using data collected from two different sensor systems with different IFOVs, for example, Landsat TM data (30×30 m) for Date 1 and SPOT HRV XS data (20×20 m) for Date 2. In such cases, it is usually necessary to decide on a representative minimum mapping unit (e.g., 20×20 m) and then resample both datasets to this uniform pixel size. This does not present a significant problem as long as the image analyst remembers that the information content of the resampled data can never be greater than the IFOV of the original sensor system (i.e., even though the Landsat TM data may be resampled to 20×20 m pixels, the information was still acquired at 30×30 m resolution and we should not expect to be able to extract additional spatial detail from the dataset).

Geometric rectification algorithms discussed in Chapter 6 are used to register the images to a standard map projection (Universal Transverse Mercator for most U.S. projects). Rectification should result in the two images having a root mean square error (RMSE) of ≤ 0.5 pixel. Misregistration of the two images may result in the identification of spurious areas of change between the datasets. For example, just one pixel misregistration may cause a stable road on the two dates to show up as a new road in the change image. Gong et al. (1992) suggest that adaptive grayscale mapping (a form of spatial filtering) be used in certain instances to remove change detection misregistration noise.

Some remote sensing systems like SPOT, IKONOS, and QuickBird collect data at off-nadir *look angles* as much as ±20°; that is, the sensors obtain data of an area on the ground from an *oblique* vantage point. Two images with significantly different look angles can cause problems when used for change detection purposes. For example, consider a maple forest consisting of very large, randomly spaced trees. A SPOT image acquired at 0° off-nadir will look directly down on the top of the canopy. Conversely, a SPOT image acquired at 20° off-nadir will record reflectance information from the side of the canopy. Differences in reflectance from the two datasets may cause spurious change detection results. Therefore, the data used in a remote sensing digital change detection should be acquired with approximately the same look angle, if possible.

Spectral Resolution

A fundamental assumption of digital change detection is that a difference exists in the spectral response of a pixel on two dates if the biophysical materials within the IFOV have changed between dates. Ideally, the spectral resolution of the remote sensor system is sufficient to record reflected radiant flux in spectral regions that best capture the most descriptive spectral attributes of the object. Unfortunately, different sensor systems do not record energy in exactly the same portions of the electromagnetic spectrum (i.e., bandwidths). For example, the Landsat multispectral scanner (MSS) recorded energy in four relatively broad multispectral bands. SPOT 1, 2, and 3 HRV sensors collect data in three relatively broad multispectral bands and one panchromatic band. The Landsat 7 Enhanced Thematic Mapper Plus (ETM^+) collects data in six relatively broad optical bands, one thermal infrared band, and one broad panchromatic band (Chapter 2). Ideally, the same sensor system is used to acquire imagery on multiple dates. When this is not possible, the analyst should *select bands that approximate one another.* For example, Landsat MSS bands 4 (green), 5 (red), and 7 (near-infrared) and SPOT bands 1 (green), 2 (red), and 3 (near-infrared), can be used successfully with Landsat ETM^+ bands 2 (green), 3 (red), and 4 (near-infrared). Many of the change detection algorithms do not function well when bands from one sensor system do not match those of another sensor system (e.g., utilizing the Landsat TM band 1 (blue) with either SPOT or Landsat MSS data may not be wise).

Radiometric Resolution

An analog-to-digital conversion of the satellite remote sensor data usually results in 8-bit brightness values ranging from 0 to 255 (Table 2-2). Ideally, the sensor systems collect the data at the *same radiometric precision on both dates.* When the radiometric resolution of data acquired by one system (e.g., Landsat MSS 1 with 6-bit data) is compared with data acquired by a higher radiometric resolution instrument (e.g., Landsat TM with 8-bit data), the lower-resolution data (e.g., 6 bits) should be decompressed to 8 bits for change detection purposes. The precision of decompressed

brightness values can never be better than the original, non-compressed data. Ideally, the brightness values associated with both dates of imagery are converted to apparent surface reflectance, which eliminates the problem.

Environmental Considerations of Importance When Performing Change Detection

Failure to understand the impact of various environmental characteristics on the remote sensing change detection process can lead to inaccurate results. When performing change detection, it is desirable to hold environmental variables as constant as possible.

Atmospheric Conditions

There should be no clouds (including stratus) or extreme humidity on the days that remote sensing data are collected. Even a thin haze can alter spectral signatures in satellite images enough to create the false impression of spectral change between two dates. Obviously, 0% cloud cover is preferred for satellite imagery and aerial photography. At the upper limit, cloud cover >20% is usually unacceptable. It should also be remembered that clouds not only obscure terrain, but the cloud shadow also causes major image classification problems. Areas obscured by clouds or affected by cloud shadow will filter through the entire change detection process, limiting the utility of the change detection product. Therefore, analysts must use good judgment in evaluating such factors as the specific locations affected by cloud cover and shadow and the availability of timely surrogate data for obscured areas. Substituting information derived from the interpretation of aerial photography for a cloud-shrouded area might be an option. Even when the stated cloud cover is 0%, it is advisable to browse the proposed image to confirm the cloud cover estimate.

Assuming no cloud cover, the use of anniversary dates helps to ensure general, seasonal agreement between the atmospheric conditions on the two dates. However, if dramatic differences exist in the atmospheric conditions on the *n* dates of imagery to be used in the change detection process, it may be necessary to *remove the atmospheric attenuation in the imagery.* Radiative transfer-based atmospheric correction algorithms may be used to radiometrically correct the remote sensor data (Kim and Elman; 1990; Song et al., 2001). For mountainous areas, topographic effects may also have to be removed (Civco, 1989). If it is not possible to perform an absolute radiometric correction, then image-to-image normalization might be a viable alternative as discussed in Chapter 6 (Eckhardt et al., 1990; Jensen et al., 1995; Du et al., 2002).

Soil Moisture Conditions

Ideally, *the soil moisture conditions should be identical* for the *n* dates of imagery used in a change detection project. Extremely wet or dry conditions on one of the dates can cause serious change detection problems. Therefore, when selecting the remotely sensed data to be used for change detection, it is very important not only to look for anniversary dates, but also to review precipitation records to determine how much rain or snow fell in the days and weeks prior to remote sensing data collection. When soil moisture differences between dates are significant for only certain parts of the study area (perhaps due to a local thunderstorm), it may be necessary to stratify (cut out) those affected areas and perform a separate change detection analysis, which can be added back in the final stages of the project.

Phenological Cycle Characteristics

Natural ecosystems go through repeatable, predictable cycles of development. Human beings often modify the landscape in repeatable, predictable stages. These cycles of predictable development are often referred to as phenomenological or *phenological cycles*. Image analysts use these cycles to identify when remotely sensed data should be collected to obtain the maximum amount of usable change information. Therefore, analysts must be intimately familiar with the *biophysical* characteristics of the vegetation, soils, and water constituents of ecosystems and their phenological cycles. Likewise, it imperative that they understand the phenological cycles associated with human-made development, such as residential expansion at the urban/rural fringe.

Vegetation Phenology: Vegetation grows according to relatively predictable diurnal, seasonal, and annual phenological cycles. Obtaining near-anniversary images greatly minimizes the effects of seasonal phenological differences that may cause spurious change to be detected in the imagery. When attempting to identify change in agricultural crops, the analyst must be aware of when the crops were planted. Ideally, monoculture crops (e.g., corn, wheat) *are planted at approximately the same time of year* on the two dates of imagery. A month lag in planting date between fields of the same crop can cause serious change detection error. Second, the monoculture crops should be *the same species.* Different species of a crop can cause the crop to reflect energy differently on the multiple dates of anniversary imagery. In addition, changes in row spacing and direction can have an impact. These observations suggest that the analyst must

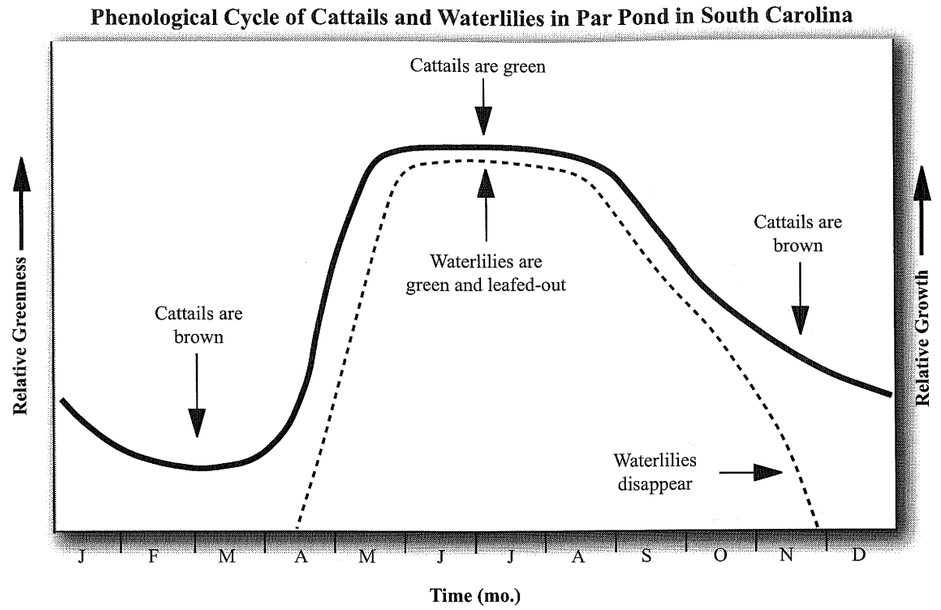

Figure 12-2 Yearly phenological cycle of cattails and waterlilies in Par Pond, SC.

know the crop's *biophysical* characteristics as well as the *cultural* land-tenure practices in the study area so that the most appropriate remotely sensed data can be selected for change detection.

Natural vegetation ecosystems such as wetland aquatic plants, forests, and rangeland have unique phenological cycles. For example, consider the phenological cycle of cattails and waterlilies found in lakes in the southeastern United States (Figure 12-2). Cattails persist year round in lakes and are generally found in shallow water adjacent to the shore (Jensen et al., 1993b). They begin greening up in early April and often have a full, green canopy by late May. Cattails senesce in late September to early October, yet they are physically present and appear brown through the winter months. Conversely, waterlilies and other nonpersistent species do not live through the winter. They appear at the outermost edge of the cattails in early May and reach full emergence 6 to 8 weeks later. The waterlily beds usually persist above water until early November, at which time they disappear. The phenological cycles of cattails and waterlilies dictate the most appropriate times for remote sensing data acquisition. The spatial distribution of cattails is best derived from remotely sensed data acquired in the early spring (April or early May) when the waterlilies have not yet developed. Conversely, waterlilies do not reach their full development until the summer, thus dictating late summer or early fall as a better period for remote sensing data acquisition and measurement. It will be shown later in this chapter that SPOT panchromatic imagery collected in April and October of most years may be used to identify change in the spatial distribution of these species in southeastern lakes.

Urban–Suburban Phenological Cycles: Urban-suburban landscapes also have phenological cycles. For example, consider the residential development from 1976 to 1978 in the 6-mi^2 portion of the Fitzsimmons 7.5-minute quadrangle near Denver, CO. Aerial photographs obtained on October 8, 1976, and October 15, 1978, reveal dramatic changes in the landscape (Figures 12-3). Most novice image analysts assume that change detection in the urban–rural fringe will capture the residential development in the two most important stages: rural undeveloped land and completely developed residential. Jensen (1981) identified 10 stages of residential development taking place in this region based on evidence of clearing, subdivision, transportation, buildings, and landscaping (Figure 12-4). The remotely sensed data will most likely capture the development in all 10 stages of development. Many of these stages may appear spectrally similar to other phenomena. For example, it is possible that stage 10 pixels (subdivided, paved roads, building, and completely landscaped) may look exactly like stage 1 pixels (original land cover) in multispectral feature space if a relatively coarse spatial resolution sensor system such as the Landsat MSS (79 × 79 m) is used. This can cause serious change detection problems. Therefore, the analyst must be intimately aware of the phenological cycle of all urban phenomena being investigated, as well as the natural ecosystems.

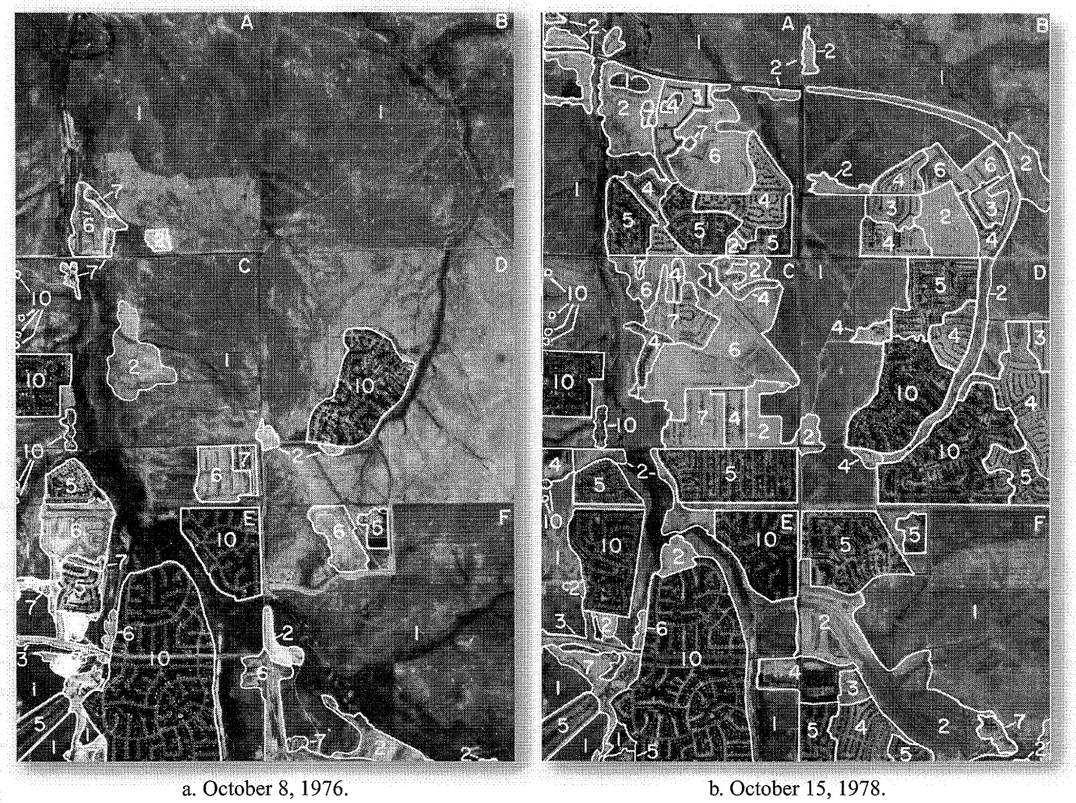

a. October 8, 1976. b. October 15, 1978.

Figure 12-3 a) Panchromatic aerial photograph of a portion of the Fitzsimmons 7.5-minute quadrangle near Denver, CO, on October 8, 1976. The original scale was 1:52,800. The land cover was visually photo-interpreted and classified into 10 classes of residential development using the logic shown in Figure 12-4. b) Panchromatic aerial photograph of a portion of the Fitzsimmons 7.5-minute quadrangle on October 15, 1978. The original scale was 1:57,600. Comparison with the 1976 aerial photograph reveals substantial residential land development since October 8, 1976.

Effects of Tidal Stage on Change Detection

Tidal stage is a crucial factor when conducting change detection in the coastal zone. Ideally, the tidal stage is identical on multiple-date images used for change detection. Sometimes this severe constraint can rule out the use of satellite remote sensing systems that cannot collect data off-nadir to meet the stringent tidal requirements. In such cases, the only way to obtain remote sensor data in the coastal zone that meets the stringent tidal requirements is to use suborbital sensors that can be flown at the exact time required. For most regions,

Dichotomous Key Used to Identify Progressive Stages of Residential Development

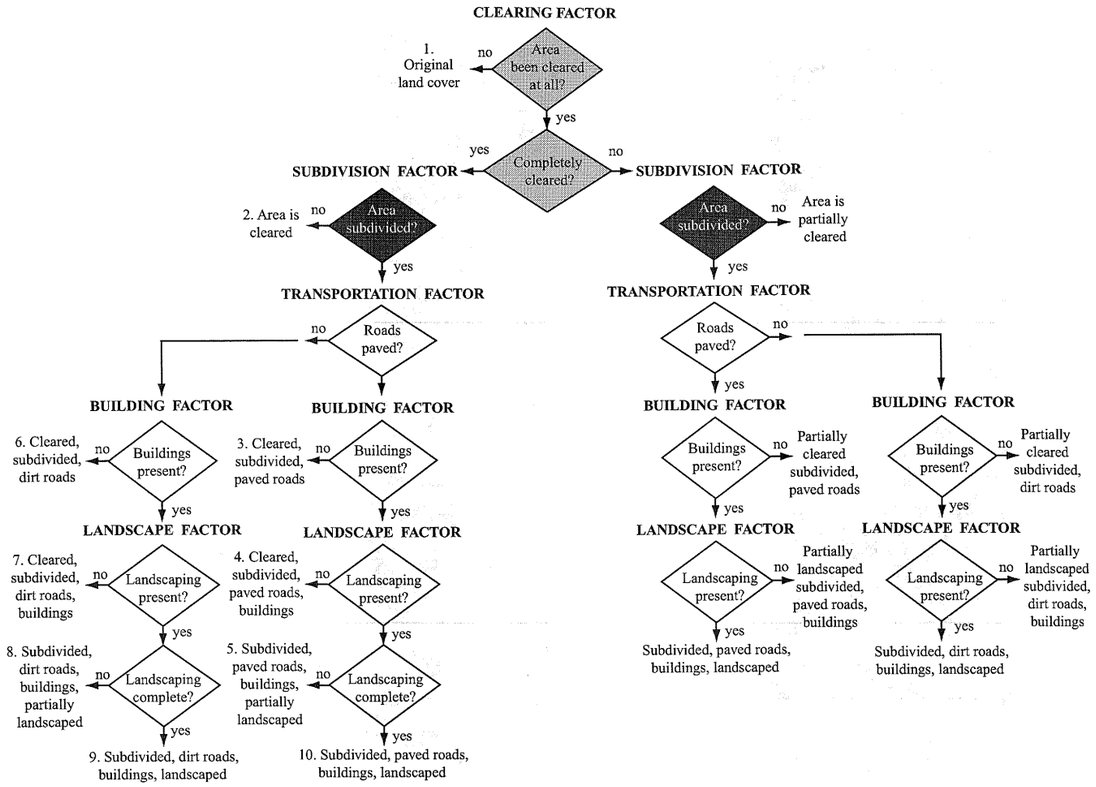

Figure 12-4 Dichotomous key used to identify progressive stages of residential development. Such development in Denver, CO, normally begins by clearing the terrain of vegetation prior to subdivision. In many geographic areas, such as the eastern and southeastern United States, however, some natural vegetation is usually left as landscaping. The absence or existence of natural vegetation dramatically affects the range of signatures that a parcel of land undergoes as it progresses from natural vegetation (1) to fully landscaped residential housing (10).

images to be used for change detection acquired at mean low tide (MLT) are preferred, 1 or 2 ft above MLT are acceptable, and 3 ft or more are generally unacceptable (Jensen et al., 1993a).

Selection of a Change Detection Algorithm

The selection of an appropriate change detection algorithm is very important (Jensen et al., 1995; 2002). First, it will have a direct impact on the type of image classification to be performed (if any). Second, it will dictate whether important "from–to" change information can be extracted from the imagery. Many change detection projects require that "from–to" information be readily available in the form of maps and tabular summaries. Change detection algorithms commonly used include:

- write function memory insertion
- multi-date composite image
- image algebra (e.g., band differencing, band ratioing)
- post-classification comparison

- binary mask applied to date 2
- ancillary data source used as date 1
- spectral change vector analysis
- chi-square transformation
- cross-correlation
- visual on-screen digitization
- knowledge-based vision systems.

It is instructive to review these change detection alternatives and provide specific examples where appropriate.

Change Detection Using Write Function Memory Insertion

A simple yet powerful method of *visual* change detection involves the use of the three write function memory (WFM) banks found on the graphics card of every digital image processing system (see Chapters 3 and 5). Basically, individual bands (or derivative products) from multiple dates may be inserted into each of the three WFM banks (red, green, or blue) (Figure 12-5) to identify change in the imagery. To appreciate the technique, consider the change that has taken place on the shoreline of Lake Mead, NV. Lake Mead's watershed had experienced a severe drought for the past 5 years, resulting in a significant drawdown of the lake. Figure 12-6a depicts Landsat ETM$^+$ imagery (band 4; 0.75 – 0.90 μm) obtained on May 3, 2000. Figure 12-6b is an ASTER image (band 3; 0.76 – 0.86 μm) of the same geographic area obtained on April 19, 2003. Color versions of these two images are found in **Color Plate 12-1a,b**. Note that both datasets record approximately the same near-infrared radiant flux and that the images are within 14 days of being anniversary dates. The ETM$^+$ and ASTER images were resampled to 30 × 30 m (nearest-neighbor; RMSE ± 0.5 pixel).

It is possible using write function memory insertion to view multiple dates of registered imagery at one time on the display screen to highlight changes. For example, **Color Plate 12-1c** is a WFM insertion change detection that highlights the land exposed by the drawdown of Lake Mead. It was produced by placing the 2003 ASTER image (band 3; 0.76 – 0.86 μm) in the red image plane and the 2000 ETM$^+$ image (band 4; 0.75 – 0.90 μm) in both the green and blue memory planes, respectively. The result is a dramatic display of the area that has changed from 2000 to 2003 highlighted in red.

Write Function Memory Insertion Change Detection

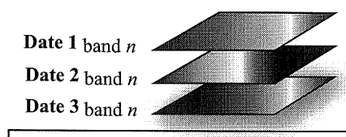

Advantages	Disadvantages
* Visual examination of 2 or 3 years of nonspecific change	* Nonquantitative
* Does not normally require atmospheric correction	* No "from–to" change class information

Figure 12-5 Advantages and disadvantages of write function memory insertion change detection.

Placing the 2003 ASTER image in the green function memory plane and the 2000 ETM$^+$ data in the red and blue image memory planes results in the change being displayed in shades of green (not shown).

WFM insertion may be used to visually examine virtually any type of registered, multiple-date information. For example, Franklin et al. (2002) placed Landsat TM Kauth-Thomas wetness index images from different years in the red, green, and blue function memories to visually highlight forest structure changes.

Advantages of write function memory insertion change detection include the possibility of looking at two and even three dates of remotely sensed imagery (or derivative products) at one time. Also, it is generally not necessary to atmospherically correct the remote sensor data used in write function memory insertion (unless the data are NDVI-related). Unfortunately, the technique does not provide quantitative information on the amount of hectares changing *from* one land-cover category *to* another. Nevertheless, it is an excellent analog method for qualitatively assessing the amount of change in a region, which might help with the selection of one of the more quantitative change detection techniques.

Multidate Composite Image Change Detection

Numerous researchers have rectified multiple dates of remotely sensed imagery (e.g., selected bands of two IKONOS scenes of the same region) and placed them in a single dataset (Figure 12-7). This composite dataset can then be analyzed in a number of ways to extract change information. First, a traditional classification using all *n* bands (six in

Multiple-Date Composite Image Change Detection Based on Principal Components Analysis

Lake Mead, NV, dataset consists of
* Landsat ETM$^+$ data obtained on May 3, 2000 (bands 2, 3, 4)
* ASTER data obtained on April 19, 2003 (bands 1, 2, 3)

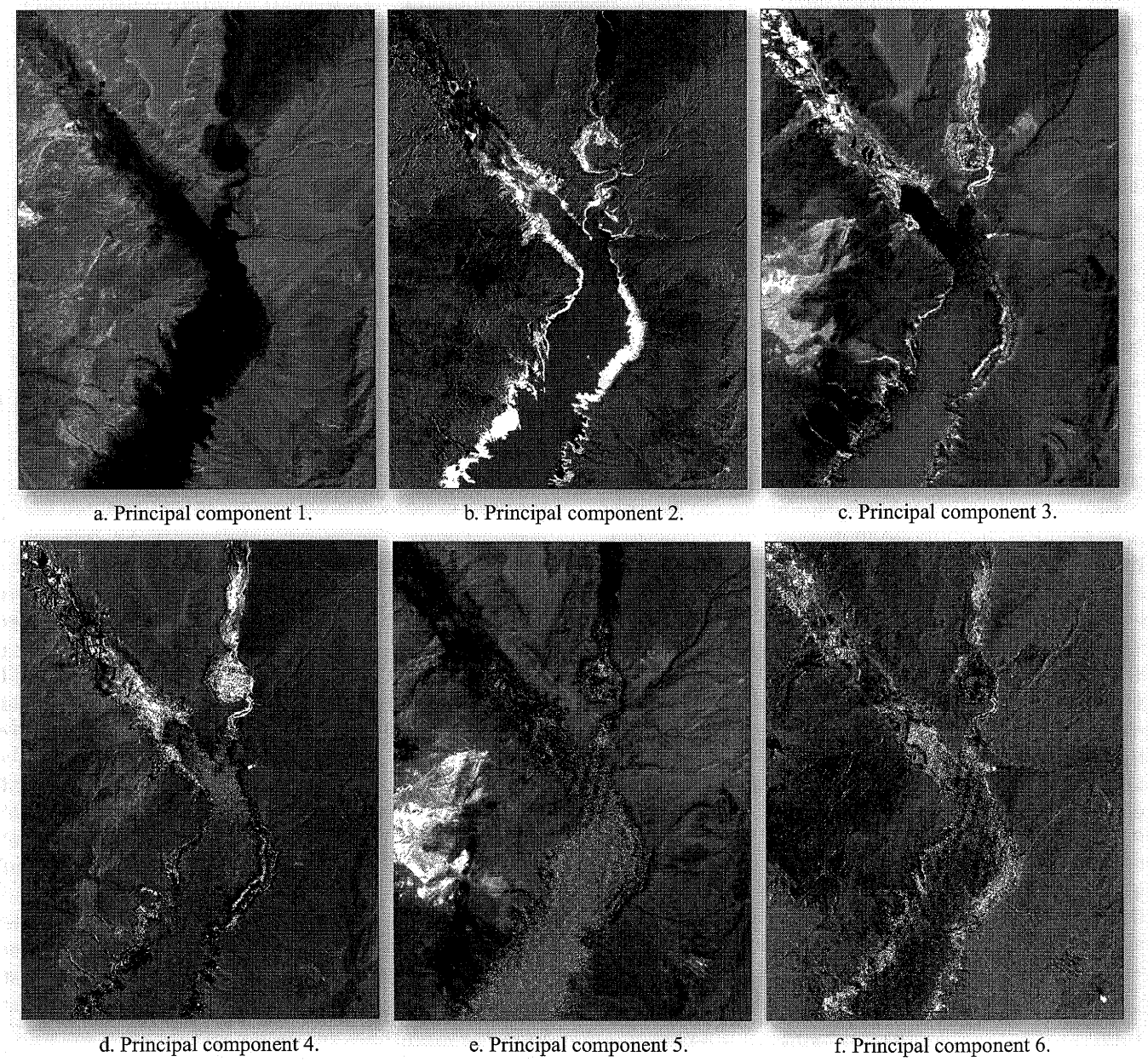

a. Principal component 1. b. Principal component 2. c. Principal component 3.

d. Principal component 4. e. Principal component 5. f. Principal component 6.

Figure 12-8 Principal components derived from a multiple-date dataset consisting of Landsat ETM$^+$ and ASTER imagery. Principal component 2 contains change information. The first three principal components were placed in various write function memory banks to highlight more subtle changes, as shown in **Color Plate 12-2**.

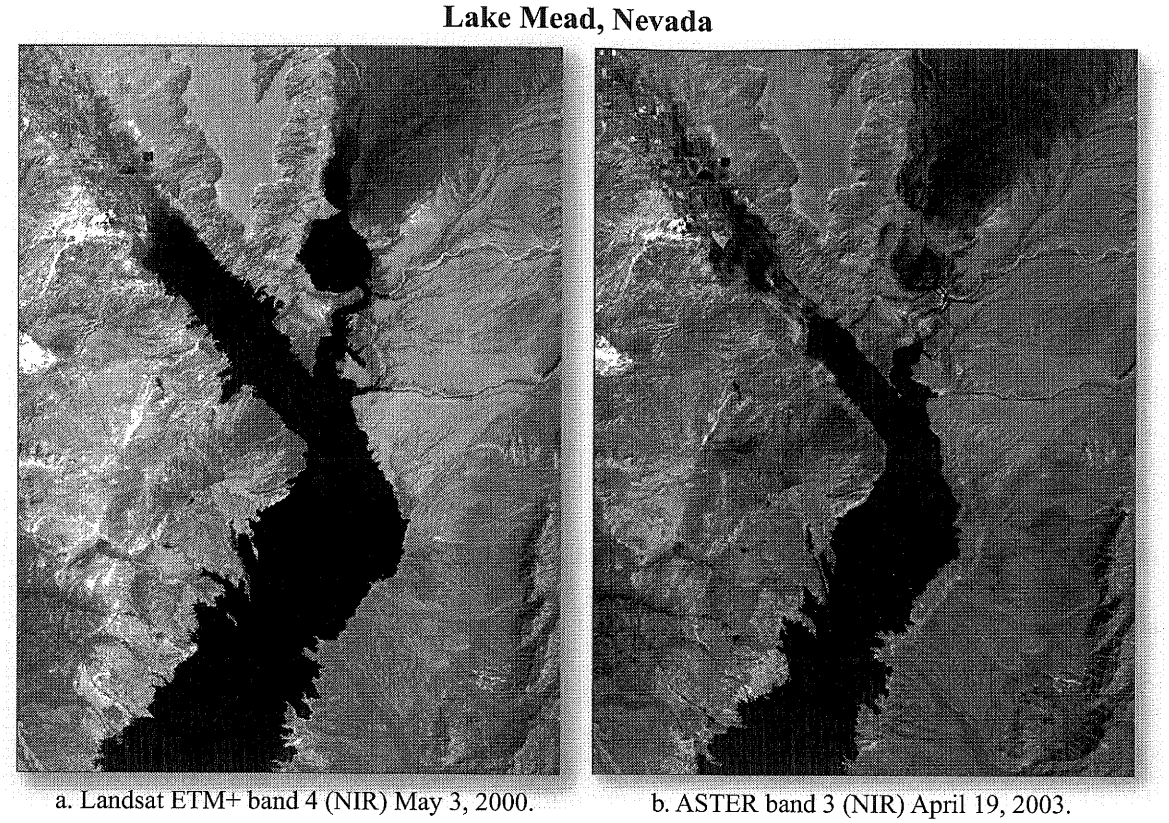

Figure 12-6 a) Landsat ETM+ imagery of a portion of Lake Mead in Nevada obtained on May 3, 2000. b) ASTER data of Lake Mead obtained on April 19, 2003 (images courtesy NASA Earth Observatory).

the example in Figure 12-7) may be performed. Unsupervised classification techniques will result in the creation of change and no-change clusters. The analyst must then label the clusters accordingly.

Other researchers have subjected the registered composite image dataset to principal component analysis (PCA) to detect change (Fung and LeDrew, 1988; Eastman and Fulk, 1993; Bauer et al., 1994; Yuan and Elvidge, 1998; Maas, 1999). A PCA based on variance–covariance matrices or a standardized PCA based on analysis of correlation matrices is then performed. This results in the computation of eigenvalues and factor loadings used to produce a new, uncorrelated PCA image dataset. The major components of the derived PCA dataset tend to account for variation in the image data that is *not* due to land-cover change, and they are termed *stable components*. Minor components tend to enhance spectral contrasts between the two dates, and they are termed *change components* (Collins and Woodcock, 1996). The difficulty arises when trying to interpret and

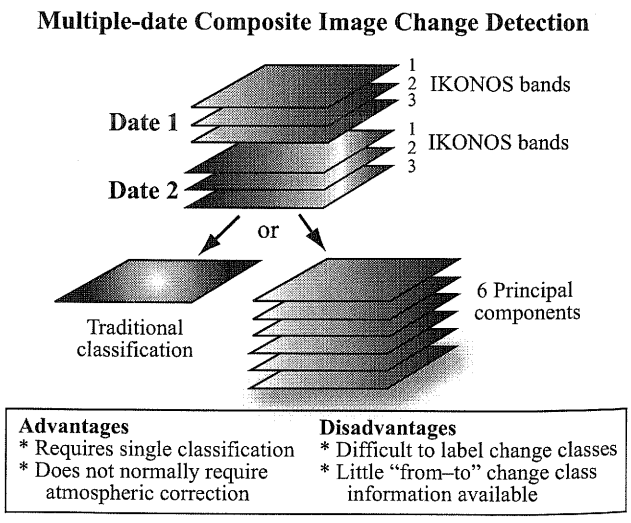

Figure 12-7 Diagram of multiple-date composite image change detection.

label each component image. Nevertheless, the method is of value and is used frequently. The advantage of this technique is that data do not have to be atmospherically corrected and only a single classification is required. Unfortunately, it is often difficult to label the change classes, and from–to change class information may not be available.

An example of a multiple-date composite image change detection is shown in Figure 12-8. The two three-band Lake Mead, NV, datasets (Landsat ETM$^+$ and ASTER) were merged into a single six-band dataset and subjected to a principal components analysis. This resulted in the creation of the six principal component images shown in Figure 12-8. Note that principal component 2 is a *change component image* (Figure 12-8b) containing detailed information about the area exposed by the lake drawdown. More subtle change information can be visually extracted from the multiple-date component dataset by placing the first three principal components in various write function memory banks, as shown in **Color Plate 12-2**.

Image Algebra Change Detection

It is possible to identify the amount of change between two rectified images by band ratioing or image differencing (Green et al., 1994; Maas, 1999; Song et al., 2001). Image differencing involves subtracting the imagery of one date from that of another (Figure 12-9). If the two images have almost identical radiometric characteristics (i.e., the data have been normalized or atmospherically corrected), the subtraction results in positive and negative values in areas of radiance change and zero values in areas of no change. The results are stored in a new change image. When 8-bit data are analyzed in this manner, the potential range of difference values found in the change image is –255 to 255 (Figure 12-10). The results can be transformed into positive values by adding a constant, c (e.g., 127). The operation is expressed as:

$$\Delta BV_{ijk} = BV_{ijk}(1) - BV_{ijk}(2) + c \qquad (12\text{-}1)$$

where

ΔBV_{ijk} = change pixel value
$BV_{ijk}(1)$ = brightness value on date 1
$BV_{ijk}(2)$ = brightness value on date 2
c = a constant (e.g., 127)
i = line number
j = column number
k = a single band (e.g., IKONOS band 3).

The change image produced using image differencing usually yields a BV distribution approximately Gaussian, where

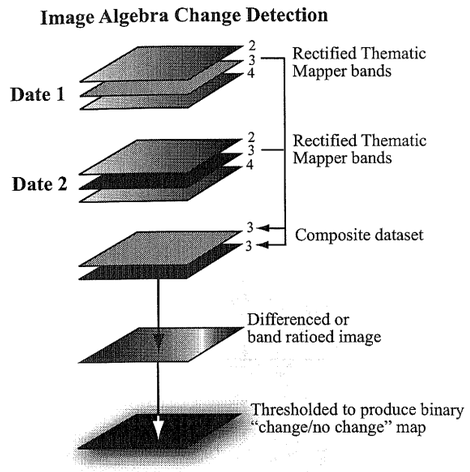

Advantages	Disadvantages
* Normally does not require atmospheric correction	* No "from–to" change information available
* Efficient method of identifying pixels that have changed in brightness value between dates	* Requires careful selection of the "change/no change" threshold

Figure 12-9 Diagram of image algebra change detection.

pixels of no BV change are distributed around the mean and pixels of change are found in the tails of the distribution (Song et al., 2001). It is not necessary to add the constant c in Equation 12-1 if the image differencing output file is allowed to be floating point, i.e., the differenced pixel values can range from –255 to 255 (Figure 12-10). Band ratioing involves exactly the same logic, except a ratio is computed with values ranging from $\frac{1}{255}$ to 255 and the pixels that did not change have a ratio value of 1 in the change image.

Image differencing change detection will be demonstrated using two datasets. The first example involves the Landsat ETM$^+$ imagery (band 4; 0.75 – 0.90 µm) obtained on May 3, 2000, and the ASTER imagery (band 3; 0.76 – 0.86 µm) of Lake Mead obtained on April 19, 2003 (Figure 12-11a and b). These two images were differenced, resulting in the change image histogram shown in Figure 12-11c. Note that the change image histogram is symmetrical, suggesting that one image was histogram-matched to the other. Note that most of the scene did not change between 2000 and 2003; therefore, the vast majority of the pixels are found around the value 0 in the histogram. However, where the lake was drawn down, exposing bedrock, and where new vegetation has grown on the exposed terrain has resulted in significant change documented in the change image in Figure 12-11d.

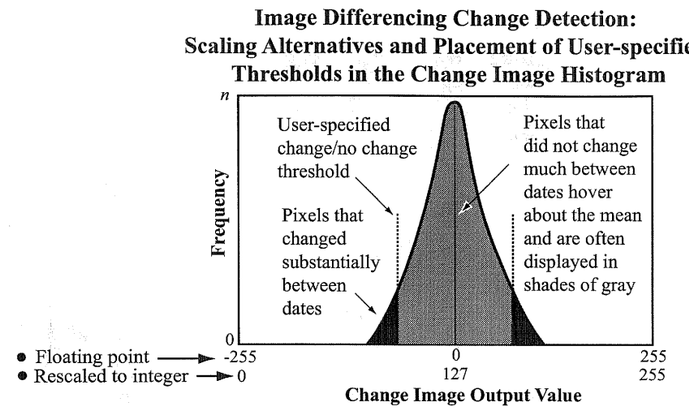

Figure 12-10 Image differencing change detection using two dates of 8-bit remote sensor data results in an output change image that can range from –255 to 255. The entire data range may be preserved if the data are stored in floating point format. The data may also be rescaled to 8-bit (0 to 255) data using Equation 12-1 and a constant. Pixels that had approximately the same brightness value (or reflectance if the data were radiometrically corrected) on both dates will produce change image pixel values that hover around 0 or 127, depending upon the scaling. Pixel values that changed dramatically between the two dates will show up in the tails of the change image histogram. Analysts can highlight certain types of change by identifying thresholds in one or both of the tails in the change image. The user-specified thresholds are usually not symmetrical about the mean.

There are actually two types of change in Figure 12-11d, bright white and black. All pixels in the change histogram below the first analyst-specified threshold were assigned black and all those above the second threshold were assigned white. The effect is even more dramatic when these two types of change are color-coded red and green, as shown in **Color Plate 12-1d**.

Figure 12-12 depicts the result of performing image differencing on April 26, 1989, and October 4, 1989, SPOT panchromatic imagery of Par Pond in South Carolina (Jensen et al., 1993b). The data were rectified, normalized, and masked using the methods previously described. The two files were then differenced and a change detection threshold was selected. The result was a change image showing the waterlilies that grew from April 26, 1989, to October 4, 1989 highlighted in gray (Figure 12-12c). The hectares of waterlily change are easily computed. Such information is used to evaluate the effect of various industrial activities on inland wetland habitat.

A critical element of both image differencing and band ratioing change detection is deciding where to place the threshold boundaries between "change" and "no-change" pixels displayed in the change image histogram. The threshold boundaries are rarely known a priori, but have to be found empirically. Sometimes a standard deviation from the mean is selected and tested. Conversely, most analysts prefer to experiment empirically, placing the threshold at various locations in the tails of the distribution until a realistic amount of change is encountered (Figures 12-10 and 12-11). Thus, the amount of change selected and eventually recoded for display is often subjective and must be based on familiarity with the study area. Unfortunately, image differencing simply identifies the areas that may have changed and provides no "from–to" change information. Nevertheless, the technique is valuable when used in conjunction with other techniques such as the multiple-date change detection using a binary change mask.

Differencing Vegetation Index Images: Image differencing does not have to be based on just the individual bands of remote sensor data. It may also be extended to comparing vegetation index information derived from multiple dates of imagery. For example, scientists have computed a normalized difference vegetation index (NDVI) on two dates and then subtracted one from another to determine change (Yuan and Elvidge, 1998; Lyon et al., 1998; Song et al., 2001):

$$\Delta NDVI_{ij} = NDVI_{ij}(1) - NDVI_{ij}(2) + c, \qquad (12\text{-}2)$$

where

$\Delta NDVI_{ij}$ = change in NDVI value
$NDVI_{ij}(1)$ = NDVI value on Date 1
$NDVI_{ij}(2)$ = NDVI value on Date 2

Image Differencing Change Detection of Waterlily Growth on Par Pond in South Carolina

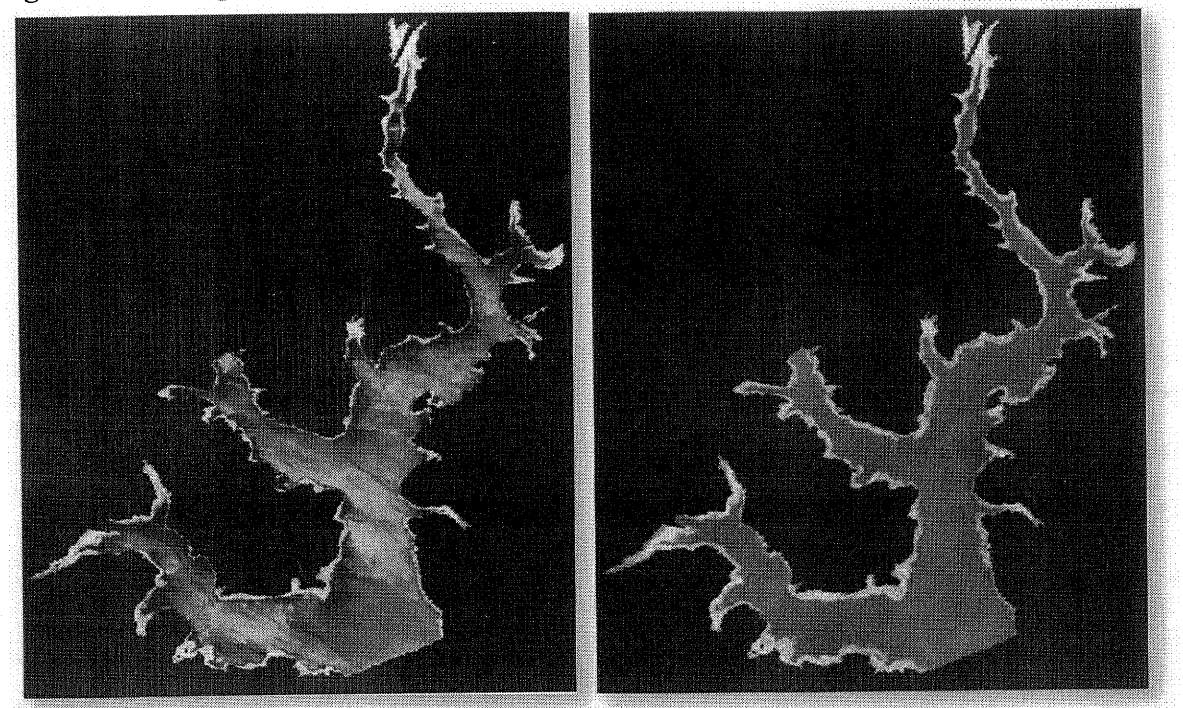

a. SPOT panchromatic image April 26, 1989.

b. SPOT panchromatic image October 4, 1989.

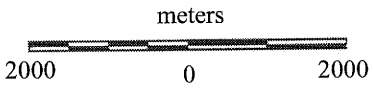

c. Waterlily growth from April 26, 1989, to October 4, 1989, identified using image differencing change detection.

Figure 12-12 a) Rectified and masked SPOT panchromatic data of Par Pond located on the Savannah River Site in South Carolina obtained on April 26, 1989. b) SPOT panchromatic data of Par Pond located on the Savannah River Site in South Carolina obtained on October 4, 1989. c) A map depicting the change in waterlilies from April 26, 1989, to October 4, 1989, using image differencing logic (Jensen et al., 1993b).

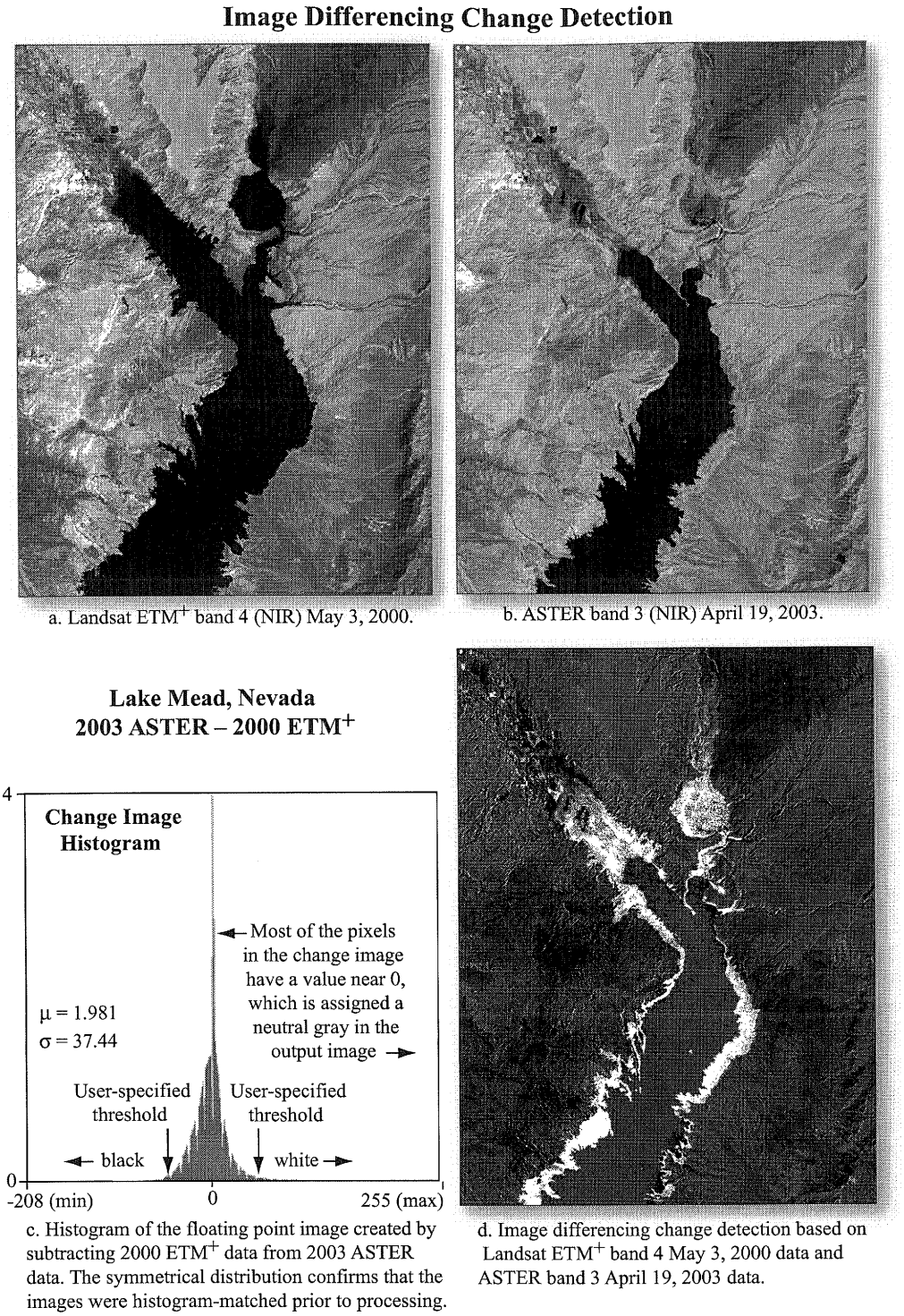

Figure 12-11 a) Landsat ETM+ imagery of a portion of Lake Mead in Nevada obtained on May 3, 2000. b) ASTER data of Lake Mead obtained on April 19, 2003. (c) The histogram of a change image produced by subtracting the ETM+ 2000 data from the ASTER 2003 data. d) Map showing the change as a function of the two thresholds identified in the change image histogram. Values near 0 are shown in shades of gray. Values below the threshold are in black and those above the threshold are in white (images courtesy NASA Earth Observatory).

i = line number
j = column number
c = a constant.

It is not necessary to use the constant c in Equation 12-2 if the image differencing output file is allowed to be floating point. The individual images used to perform NDVI change detection should be atmospherically corrected. Change detection based on differencing multiple-date Kauth-Thomas transformations (e.g., change in brightness, greenness, and/or wetness) have also been widely adopted (Ridd and Liu, 1998; Franklin et al., 2002).

Post-classification Comparison Change Detection

Post-classification comparison change detection is a heavily used quantitative change detection method (e.g., Jensen et al., 1995; 2002; Yuan and Elvidge, 1998; Maas, 1999; Song et al., 2001; Civco, 2002; Arzandeh and Wang, 2003). It requires rectification and classification of each remotely sensed image (Figure 12-13). The two maps are then compared on a pixel-by-pixel basis using a *change detection matrix,* to be discussed. Unfortunately, every error in the individual date classification map will also be present in the final change detection map (Rutchey and Velcheck, 1994). Therefore, it is imperative that the individual classification maps used in the post-classification change detection method be as accurate as possible (Arzandeh and Wang, 2003).

To demonstrate the post-classification comparison change detection method, consider the Kittredge (40 river miles inland from Charleston, SC) and Fort Moultrie, SC, study areas (Jensen et al., 1993a) (**Color Plate 12-3**). Nine land-cover classes were inventoried on each date (**Color Plate 12-4**). The 1982 and 1988 classification maps were then compared on a pixel-by-pixel basis using an $n \times n$ GIS matrix algorithm whose logic is shown in **Color Plate 12-5a**. This resulted in the creation of a change image map consisting of brightness values from 1 to 81. The analyst then selected specific "from–to" classes for emphasis. Only a select number of the 72 possible off-diagonal "from–to" land-cover change classes summarized in the change matrix (**Color Plate 12-5a**) were selected to produce the change detection maps (**Color Plate 12-6a** and **b**). For example, all pixels that changed from any land cover in 1982 to Developed Land in 1988 were color coded red (RGB = 255, 0, 0) by selecting the appropriate "from–to" cells in the change detection matrix (10, 19, 28, 37, 46, 55, 64, and 73). Note that the change classes are draped over a Landsat TM band 4 image of the study area to facilitate orientation. Similarly, all

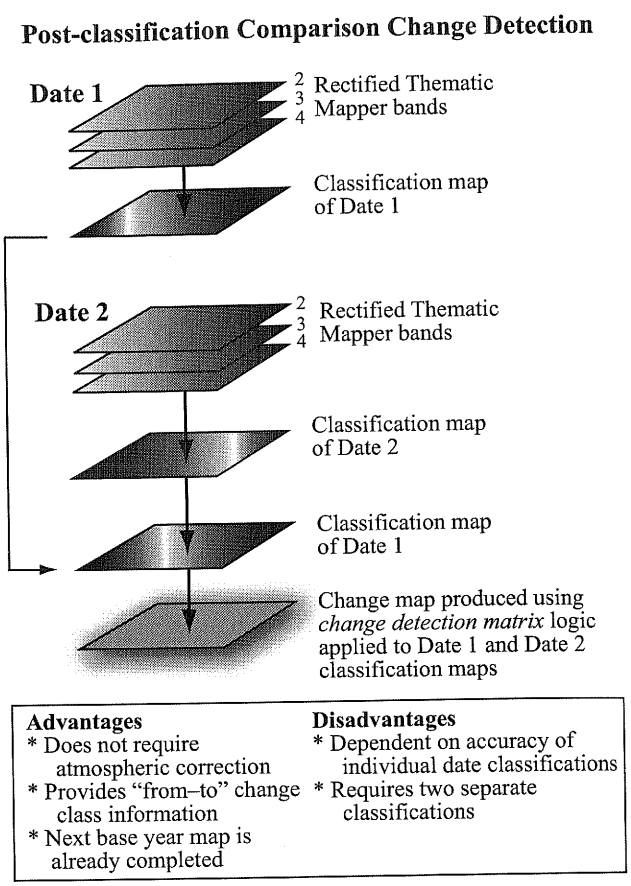

Figure 12-13 Diagram of post-classification comparison change detection.

pixels in 1982 that changed to Estuarine Unconsolidated Shore by December 19, 1988 (cells 9, 18, 27, 36, 45, 54, 63, and 72), were depicted in yellow (RGB = 255, 255, 0). If desired, the analyst could highlight very specific changes such as all pixels that changed from Developed Land to Estuarine Emergent Wetland (cell 5 in the matrix) by assigning a unique color look-up table value (not shown). A color-coded version of the change detection matrix can be used as an effective "from–to" change detection map legend.

Post-classification comparison change detection is widely used and easy to understand. When conducted by skilled image analysts, it represents a viable technique for the creation of change detection products. Advantages include the detailed "from–to" information that can be extracted and the fact that the classification map for the next base year is already complete (Arzandeh and Wang, 2003). However, the accuracy of the change detection depends on the accuracy of the two separate classification maps.

i = line number
j = column number
c = a constant.

It is not necessary to use the constant c in Equation 12-2 if the image differencing output file is allowed to be floating point. The individual images used to perform NDVI change detection should be atmospherically corrected. Change detection based on differencing multiple-date Kauth-Thomas transformations (e.g., change in brightness, greenness, and/or wetness) have also been widely adopted (Ridd and Liu, 1998; Franklin et al., 2002).

Post-classification Comparison Change Detection

Post-classification comparison change detection is a heavily used quantitative change detection method (e.g., Jensen et al., 1995; 2002; Yuan and Elvidge, 1998; Maas, 1999; Song et al., 2001; Civco, 2002; Arzandeh and Wang, 2003). It requires rectification and classification of each remotely sensed image (Figure 12-13). The two maps are then compared on a pixel-by-pixel basis using a *change detection matrix,* to be discussed. Unfortunately, every error in the individual date classification map will also be present in the final change detection map (Rutchey and Velcheck, 1994). Therefore, it is imperative that the individual classification maps used in the post-classification change detection method be as accurate as possible (Arzandeh and Wang, 2003).

To demonstrate the post-classification comparison change detection method, consider the Kittredge (40 river miles inland from Charleston, SC) and Fort Moultrie, SC, study areas (Jensen et al., 1993a) (**Color Plate 12-3**). Nine land-cover classes were inventoried on each date (**Color Plate 12-4**). The 1982 and 1988 classification maps were then compared on a pixel-by-pixel basis using an $n \times n$ GIS matrix algorithm whose logic is shown in **Color Plate 12-5a**. This resulted in the creation of a change image map consisting of brightness values from 1 to 81. The analyst then selected specific "from–to" classes for emphasis. Only a select number of the 72 possible off-diagonal "from–to" land-cover change classes summarized in the change matrix (**Color Plate 12-5a**) were selected to produce the change detection maps (**Color Plate 12-6a** and **b**). For example, all pixels that changed from any land cover in 1982 to Developed Land in 1988 were color coded red (RGB = 255, 0, 0) by selecting the appropriate "from–to" cells in the change detection matrix (10, 19, 28, 37, 46, 55, 64, and 73). Note that the change classes are draped over a Landsat TM band 4 image of the study area to facilitate orientation. Similarly, all

Post-classification Comparison Change Detection

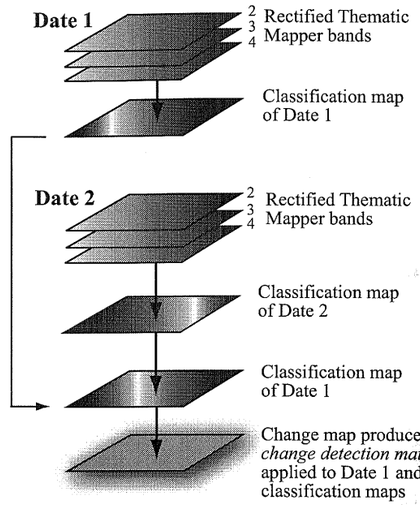

Advantages	Disadvantages
* Does not require atmospheric correction	* Dependent on accuracy of individual date classifications
* Provides "from–to" change class information	* Requires two separate classifications
* Next base year map is already completed	

Figure 12-13 Diagram of post-classification comparison change detection.

pixels in 1982 that changed to Estuarine Unconsolidated Shore by December 19, 1988 (cells 9, 18, 27, 36, 45, 54, 63, and 72), were depicted in yellow (RGB = 255, 255, 0). If desired, the analyst could highlight very specific changes such as all pixels that changed from Developed Land to Estuarine Emergent Wetland (cell 5 in the matrix) by assigning a unique color look-up table value (not shown). A color-coded version of the change detection matrix can be used as an effective "from–to" change detection map legend.

Post-classification comparison change detection is widely used and easy to understand. When conducted by skilled image analysts, it represents a viable technique for the creation of change detection products. Advantages include the detailed "from–to" information that can be extracted and the fact that the classification map for the next base year is already complete (Arzandeh and Wang, 2003). However, the accuracy of the change detection depends on the accuracy of the two separate classification maps.

Change Detection Using a Binary Change Mask Applied to Date 2

This method of change detection is very effective. First, the analyst selects the base image referred to as Date 1 at time n. Date 2 may be an earlier image ($n - 1$) or a later image ($n + 1$). A traditional classification of Date 1 is performed using rectified remote sensor data. Next, one of the bands (e.g., band 3 in Figure 12-14) from both dates of imagery is placed in a new dataset. The two-band dataset is then analyzed using various image algebra change detection functions (e.g., band ratio, image differencing) to produce a new change image file. The analyst usually selects a threshold value to identify areas of "change" and "no change" in the new image, as discussed in the section on image algebra change detection. The change image is then recoded into a binary mask file consisting of areas that have changed between the two dates. Great care must be exercised when creating the "change/no change" binary mask (Jensen et al., 1993a).The change mask is then overlaid onto Date 2 of the analysis and only those pixels that were detected as having changed are classified in the Date 2 imagery. A traditional post-classification comparison can then be applied to yield "from–to" change information.

This method may reduce change detection errors (omission and commission) and provides detailed "from–to" change class information. The technique reduces effort by allowing analysts to focus on the small amount of area that has changed between dates. In most regional projects, the amount of actual change over a 1- to 5-year period is probably no greater than 10% of the total area. The method is complex, requiring a number of steps, and the final outcome is dependent on the quality of the "change/no change" binary mask used in the analysis. Nevertheless, this is a very useful change detection algorithm.

Change Detection Using an Ancillary Data Source as Date 1

Sometimes there exists a land-cover data source that may be used in place of a traditional remote sensing image in the change detection process. For example, the U.S. Fish and Wildlife Service conducted a National Wetland Inventory (NWI) of the United States at 1:24,000 scale. Some of these data have been digitized. Instead of using a remotely sensed image as Date 1 in a coastal change detection project, it is possible to substitute the digital NWI map of the region (Figure 12-15). In this case, the NWI map is recoded to be compatible with the classification scheme being used. Next, Date

Change Detection Using a Binary Change Mask Applied to Date 2

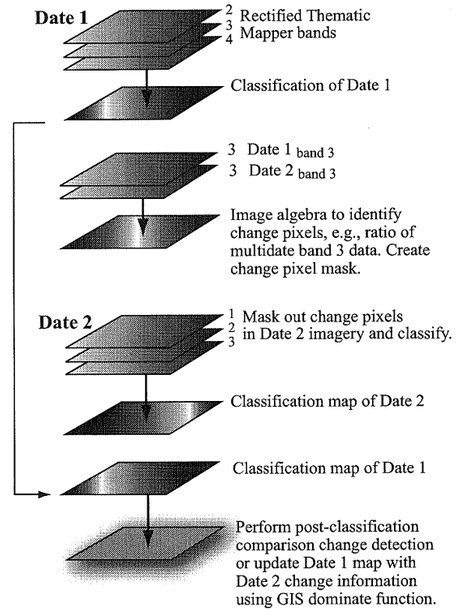

Advantages	Disadvantages
* May reduce change detection errors (omission and commission)	* Requires a number of steps
* Provides "from–to" change class information	* Dependent on quality of "change/no-change" binary mask

Figure 12-14 Diagram of change detection using a binary change mask applied to Date 2.

2 of the analysis is classified and then compared on a pixel-by-pixel basis with the Date 1 information using post-classification comparison methods. Traditional "from–to" information can then be derived.

Advantages of the method include the use of a well-known, trusted data source (e.g., NWI) and the possible reduction of errors of omission and commission. Detailed "from–to" information may be obtained using this method. Also, only a single classification of the Date 2 image is required. It may also be possible to update the NWI map (Date 1) with more current wetland information (this would be done using a GIS dominate function and the new wetland information found in the Date 2 classification). The disadvantage is that the NWI data must be digitized, generalized to be compatible with a

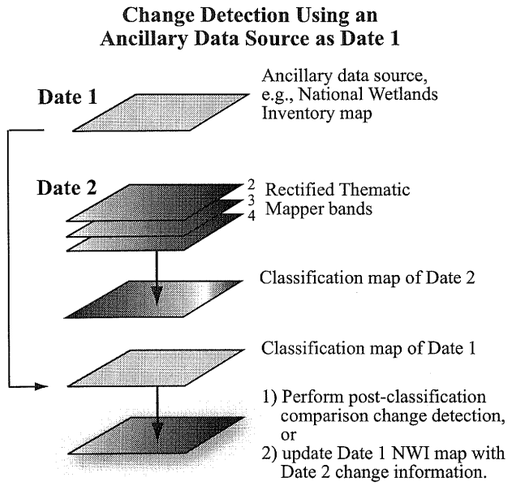

Figure 12-15 Diagram of change detection using ancillary data source as Date 1.

classification scheme, and then converted from vector to raster format to be compatible with the raster remote sensor data. Manual digitization and subsequent conversion introduce error into the database, which may not be acceptable (Lunetta et al., 1991).

Spectral Change Vector Analysis

When land undergoes a change or disturbance between two dates, its spectral appearance normally changes. For example, consider the red and near-infrared spectral characteristics of a single pixel displayed in two-dimensional feature space (Figure 12-16a). It appears that the land cover associated with this particular pixel has changed from Date 1 to Date 2 because the pixel resides at a substantially different location in the feature space on Date 2. The vector describing the direction and magnitude of change from Date 1 to Date 2 is a *spectral change vector* (Malila, 1980; Chen et al., 2003). The total change magnitude per pixel (CM_{pixel}) is computed by determining the Euclidean distance between end points through n-dimensional change space (Michalek et al., 1993):

$$CM_{pixel} = \sum_{k=1}^{n} [BV_{ijk(date2)} - BV_{ijk(date1)}]^2 \qquad (12\text{-}3)$$

where $BV_{i,j,k(date2)}$ and $BV_{i,j,k(date1)}$ are the Date 1 and Date 2 pixel values in band k.

A scale factor (e.g., 5) can be applied to each band to magnify small changes in the data if desired. The change direction for each pixel is specified by whether the change is positive or negative in each band. Thus, 2^n possible types of changes can be determined per pixel (Virag and Colwell, 1987). For example, if three bands are used there are 2^3 or 8 types of changes or sector codes possible (Table 12-1). To demonstrate, let us consider a single registered pixel measured in three bands (1, 2, and 3) on two dates. If the change in band 1 was positive (e.g., $BV_{i,j,1(date\ 2)} = 45$; $BV_{i,j,1(date\ 1)} = 38$; $BV_{change} = 45 - 38 = 7$), and the change in band 2 was positive (e.g., $BV_{i,j,2(date2)} = 20$; $BV_{i,j,2(date1)} = 10$; $BV_{change} = 20 - 10 = 10$), and the change in band 3 was negative (e.g., $BV_{i,j,3(date2)} = 25$; $BV_{i,j,3(date1)} = 30$; $BV_{change} = 25 - 30 = -5$), then the change magnitude of the pixel would be $CM_{pixel} = 7^2 + 10^2 - 5^2 = 174$, and the change sector code for this pixel would be "+, +, –" and have a value of 7, as shown in Table 12-1 and Figure 12-17. For rare instances when pixel values do not change at all between the two dates, a default direction of + may be used to ensure that all pixels are assigned a direction (Michalek et al., 1993).

Change vector analysis outputs two geometrically registered files; one contains the sector code and the other contains the scaled vector magnitudes. The change information may be superimposed onto an image of the study area with the change pixels color-coded according to their sector code. This multispectral change magnitude image incorporates both the change magnitude and direction information (Figure 12-16a). The decision that a change has occurred is made if a threshold is exceeded (Virag and Colwell, 1987). The threshold may be selected by examining deep-water areas (if present), which should be unchanged, and recording their scaled magnitudes from the change vector file. Figure 12-16b illustrates a case in which no change would be detected because the threshold is not exceeded. Conversely, change would be detected in Figures 12-16c and d because the threshold was exceeded. The other half of the information contained in the change vector, that is, its direction, is also shown in Figure 12-16c and d. Direction contains information about the type of change. For example, the direction of

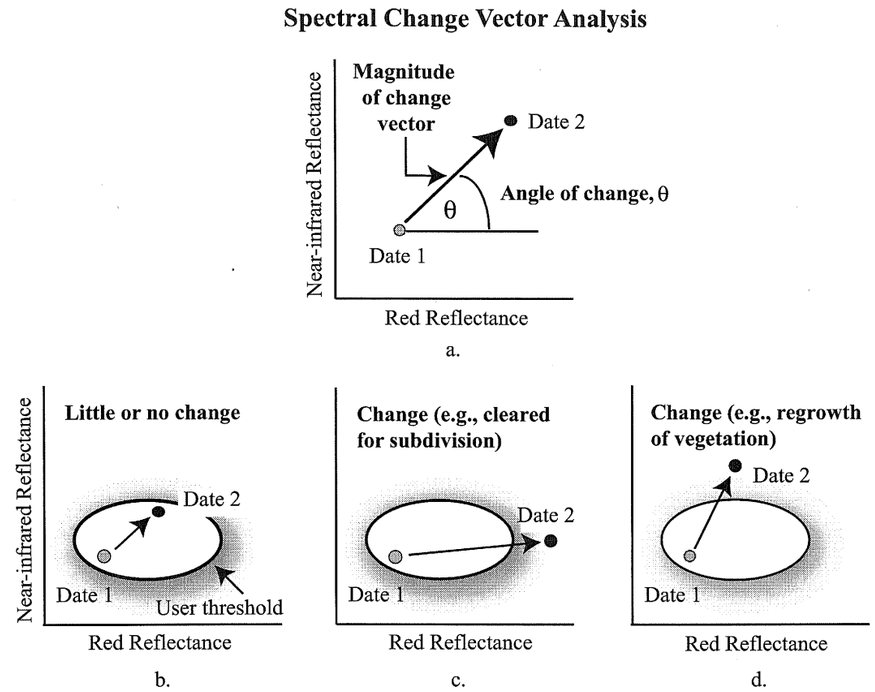

Figure 12-16 Schematic diagram of the spectral change detection method.

change due to clearing should be different from change due to regrowth of vegetation.

Change vector analysis has been applied successfully to forest change detection in northern Idaho (Malila, 1980) and for monitoring changes in mangrove and reef ecosystems along the coast of the Dominican Republic (Michalek et al., 1993). It is the change detection algorithm of choice for producing the MODIS Vegetative Cover Conversion (VCC) product being compiled on a global basis using 250 m surface reflectance data (Zhan et al., 2002). The method is based on measuring the change in reflectance in just two bands, red ($\Delta\rho_{red}$) and near-infrared ($\Delta\rho_{nir}$), between two dates and using this information to compute the change magnitude per pixel,

$$CM_{pixel} = \sqrt{(\Delta\rho_{red})^2 + (\Delta\rho_{nir})^2} \qquad (12\text{-}4)$$

and change angle (θ):

Table 12-1. Sector code definitions for change vector analysis using three bands (+ indicates pixel value increase from Date 1 to Date 2; – indicates pixel value decrease from Date 1 to Date 2) (Michalek et al., 1993).

	Change Detection		
Sector Code	Band 1	Band 2	Band 3
1	–	–	–
2	–	–	+
3	–	+	–
4	–	+	+
5	+	–	–
6	+	–	+
7	+	+	–
8	+	+	+

Spectral Change Vector Analysis

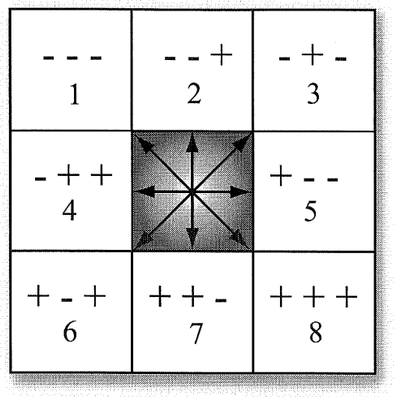

Figure 12-17 Possible change sector codes for a pixel measured in three bands on two dates.

$$\theta_{pixel} = \arctan\left(\frac{\Delta\rho_{red}}{\Delta\rho_{nir}}\right). \quad (12\text{-}5)$$

The change magnitude and angle information is then analyzed using decision-tree logic to identify important types of change in the multiple-date MODIS imagery (Zhan et al., 2002). Chen et al. (2003) developed an improved change vector analysis methodology that assists in the determination of the change magnitude and change direction thresholds when producing land-cover change maps.

Chi-square Transformation Change Detection

Ridd and Liu (1998) introduced a chi-square transformation change detection algorithm. It will work on any type of imagery but let us for the moment apply it to six bands of Landsat TM data obtained on two dates. The chi-square transformation is:

$$Y_{pixel} = (X-M)^T \Sigma^{-1} (X-M) \quad (12\text{-}6)$$

where Y_{pixel} is the digital value of the pixel in the output change image, X is the vector of the difference of the six digital values between the two dates for each pixel, M is the vector of the mean residuals of each band for the entire image, T is the transverse of the matrix, and Σ^{-1} is the inverse covariance matrix of the six bands between the two dates. The usefulness of the transformation in this context rests on the fact that Y is distributed as a chi-square random variable with p degrees of freedom where p is the number of bands. $Y = 0$ represents a pixel of no change. The user creates the output change image and highlights pixels with varying amounts of Y.

Cross-correlation Change Detection

Cross-correlation change detection makes use of an existing Date 1 digital land-cover map and a Date 2 unclassified multispectral dataset (Koeln and Bissonnette, 2000). The Date 2 multispectral dataset does not need to be atmospherically corrected or converted to percent reflectance: the original brightness values are sufficient. Several passes through the datasets are required to implement cross-correlation change detection. First, every pixel in the Date 1 land-cover map associated with a particular class c (e.g., forest) out of m possible classes is located in the Date 2 multispectral dataset (Figure 12-18). The mean (μ_{ck}) and standard deviation (σ_{ck}) of all the brightness values in each band k in the Date 2 multispectral dataset associated with class c (e.g., forest) in the Date 1 land-cover map are computed. Next, every pixel (BV_{ijk}) in the Date 2 scene associated with class c is compared with the mean (μ_{ck}) and divided by the standard deviation (σ_{ck}). This value is summed and squared over all k bands. This is performed for each class. The result is a Z-score associated with each pixel in the scene:

$$Z_{ijc} = \sum_{k=1}^{n} \left(\frac{BV_{ijk} - \mu_{c_k}}{\sigma_{c_k}}\right)^2 \quad (12\text{-}7)$$

where

Z_{ijc} is the Z-score for a pixel at location i,j in the Date 2 multispectral dataset associated with a particular class c found in the Date 1 land-cover map;

c is the Date 1 land-cover class under investigation;

n is the number of bands in the Date 2 multispectral image;

k is the band number in the Date 2 multispectral image;

BV_{ijk} is the brightness value of a pixel (or reflectance) at location i,j in band k of the Date 2 multispectral dataset associated with a particular class found in the Date 1 land-cover map;

Cross-correlation Change Detection

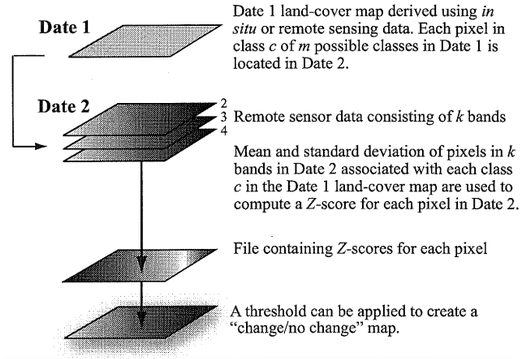

Advantages	Disadvantages
* Not necessary to atmospherically correct or normalize Date 2 image data	* Depends on quality of Date 1 classification
* Requires a single classification	* Does not provide "from–to" change class information

Figure 12-18 Diagram of cross-correlation change detection.

μ_{ck} is the mean of all pixel brightness values found in band k of the Date 2 multispectral dataset associated with a particular class c in the Date 1 land-cover map;

σ_{ck} is the standard deviation of all pixel brightness values found in band k of the Date 2 multispectral dataset associated with a particular class c in the Date 1 land-cover map.

The mean (μ_{ck}) and standard deviation (σ_{ck}) values derived from the cross-correlation of a Date 1 four-class land-cover map with a Date 2 three-band multispectral dataset would be stored in a table like Table 12-2 and used in Equation 12-7.

The Z-statistic describes how close a pixel's response is to the expected spectral response of its corresponding class value in the land-cover map (Civco et al., 2002). In the output file, the greater the Z-score of an individual pixel, the greater the probability that its land cover has changed from Date 1 to Date 2. If desired, the image analyst can examine the Z-score image file and select a threshold that can be used to identify all pixels in the scene that have changed from Date 1 to Date 2. This information can be used to prepare a "change/no change" map of the area.

Advantages associated with cross-correlation change detection include the fact that it is not necessary to perform an atmospheric correction on any dataset. It also eliminates the problems associated with phenological differences between dates of imagery. Unfortunately, this change detection method is heavily dependent upon the accuracy of the Date 1 land-cover classification. If it has serious error, then the cross-correlation between Date 1 and Date 2 will contain error. Every pixel in the Date 1 land-cover map must be assigned to a class. The method does not produce any "from–to" change detection information.

Table 12-2. Hypothetical mean and standard deviations associated with a cross-correlation change detection analysis of a Date 1 land-cover map with four classes and a Date 2 multispectral image that contains three bands.

Land Cover Class	Band 1		Band 2		Band 3	
1	$\mu_{1,1}$	$\sigma_{1,1}$	$\mu_{1,2}$	$\sigma_{1,2}$	$\mu_{1,3}$	$\sigma_{1,3}$
2	$\mu_{2,1}$	$\sigma_{2,1}$	$\mu_{2,2}$	$\sigma_{2,2}$	$\mu_{2,3}$	$\sigma_{2,3}$
3	$\mu_{3,1}$	$\sigma_{3,1}$	$\mu_{3,2}$	$\sigma_{3,2}$	$\mu_{3,3}$	$\sigma_{3,3}$
4	$\mu_{4,1}$	$\sigma_{4,1}$	$\mu_{4,2}$	$\sigma_{4,2}$	$\mu_{4,3}$	$\sigma_{4,3}$

Knowledge-based Vision Systems for Detecting Change

The use of expert systems to detect change automatically in an image with very little human interaction is still in its infancy. In fact, most scientists attempting to develop such systems have significant human intervention and employ many of the aforementioned change detection algorithms in the creation of a knowledge-based change detection vision system. For example, Wang (1993) used a preprocessor to (1) perform image differencing, (2) create a change mask (using principal components analysis), (3) perform automated fuzzy supervised classification, and (4) extract attributes. Possible urban change areas were then passed to a rule-based interpreter, which produced a change image.

Visual On-screen Change Detection and Digitization

A considerable amount of high-resolution remote sensor data is now available (e.g., IKONOS and QuickBird 1 × 1 m, U.S.G.S. National Aerial Photography Program). Much of these data are being rectified and used as planimetric base maps or orthophotomaps. Often the aerial photography data are scanned (digitized) at high resolutions into digital image files (Light, 1993). These photographic datasets can then be

registered to a common base map and compared to identify change. Digitized high-resolution aerial photography displayed on a CRT screen can be easily interpreted using standard photo interpretation techniques and the fundamental elements of image interpretation including size, shape, shadow, texture, etc. (Jensen, 2000). Therefore, it is becoming increasingly common for analysts to visually interpret both dates of aerial photography (or other type of remote sensor data) using heads-up on-screen digitizing and to compare the various images to detect change. The process is especially easy when 1) both digitized photographs (or images) are displayed on the CRT at the same time, side by side, and 2) they are topologically linked through object-oriented programming so that a polygon drawn around a feature on one photograph will also be drawn around the same object on the other photograph.

A good example of this methodology is shown in Figure 12-19. Hurricane Hugo with its 135-mph winds and 20-ft. storm surge struck the South Carolina coastline near Sullivan's Island on September 22, 1989. Vertical black-and-white aerial photographs obtained on July 1, 1988, were scanned at 500 dots per inch resolution using a Zeiss drum microdensitometer, rectified to the South Carolina State Plane Coordinate System, and resampled to 0.3×0.3 m pixels (Figure 12-19a). Aerial photographs acquired on October 5, 1989, were digitized in a similar manner and registered to the 1988 digital database (Figure 12-19b). Image analysts then performed on-screen digitization to identify the following features (Figure 12-20):

- buildings with no damage
- buildings partially damaged
- buildings completely damaged
- buildings that were moved
- buildings that might not be able to be rebuilt because they fell within certain SC Coastal Council beachfront management setback zones (base, 20-year, and 40-year)
- areas of beach erosion due to Hurricane Hugo
- areas of beach accretion due to Hurricane Hugo.

Digital classification of the digitized aerial photography on each date, performing image arithmetic (image differencing or band ratioing), or even displaying the two dates in different function memories did not work well for this type of data. The on-screen digitization procedure was the most useful for identifying housing and geomorphological change caused by Hurricane Hugo.

On-screen photo interpretation of digitized aerial photography, high-resolution aircraft multispectral scanner data, or high-resolution satellite data (e.g., SPOT panchromatic 10×10 m; QuickBird panchromatic 61×61 cm) is becoming very important for correcting or updating urban infrastructure databases. For example, the Bureau of the Census TIGER files represent a major resource for the development of GIS databases. For several reasons, the Bureau of the Census was forced to make a number of compromises during the construction of these nationwide digital cartographic files. As a result, the users of these files must develop their own procedures for dealing with some of the geometric inconsistencies in the files. One approach to solving these problems is to use remotely sensed image data as a source of current and potentially more accurate information (Cowen et al., 1991). For example, Figure 12-21a depicts U.S. Bureau of the Census TIGER road information draped over SPOT 10×10 m panchromatic data of an area near Irmo, SC. Note the serious geometric errors in the TIGER data. An analyst used heads-up, on-screen digitizing techniques to move roads to their proper planimetric positions and to add entirely new roads to the TIGER ARC-Info database (Figure 12-21b). All roads in South Carolina were updated using this type of logic and SPOT panchromatic data.

Finally, it is sometimes useful to simply visually examine multiple dates of remotely sensed imagery to appreciate processes at work. For example, consider the change in the Aral Sea in Kazakhstan from 1973 to 2000. The shoreline for a portion of the Aral Sea recorded by the Landsat MSS in 1973 and 1987 and the Landsat ETM$^+$ in 2000 is shown in **Color Plate 12-7**.

The Aral Sea is actually a lake, a body of fresh water. Unfortunately, more than 60 percent of the lake has disappeared in the last 30 years. Farmers and state offices in Uzbekistan, Kazakhstan, and Central Asian states began diverting river water to the lake in the 1960s to irrigate cotton fields and rice paddies. In 1965, the Aral Sea received about 50 cubic kilometers of fresh water per year—a number that fell to zero by the early 1980s. Concentrations of salts and minerals began to rise in the lake. The change in chemistry led to alterations in the lake's ecology, causing precipitous drops in the fish population. The commercial fishing industry employed 60,000 people in the early 1960s. By 1977, the fish harvest was reduced by 75 percent, and by the early 1980s the commercial fishing industry was gone.

Hurricane Hugo Impacts Sullivan's Island, SC, in 1989

a. Pre-Hurricane Hugo orthophotomap July 1, 1988.

b. Post-Hurricane Hugo orthophoto October 5, 1989.

Figure 12-19 a) Panchromatic orthophotomap of Sullivan's Island, SC, obtained on July 1, 1988, prior to Hurricane Hugo. The data were rectified to State Plane Coordinates and resampled to 0.3×0.3 m spatial resolution. b) Panchromatic aerial photograph of Sullivan's Island obtained on October 5, 1989, after Hurricane Hugo. The data were rectified to State Plane Coordinates and resampled to 0.3×0.3 m spatial resolution.

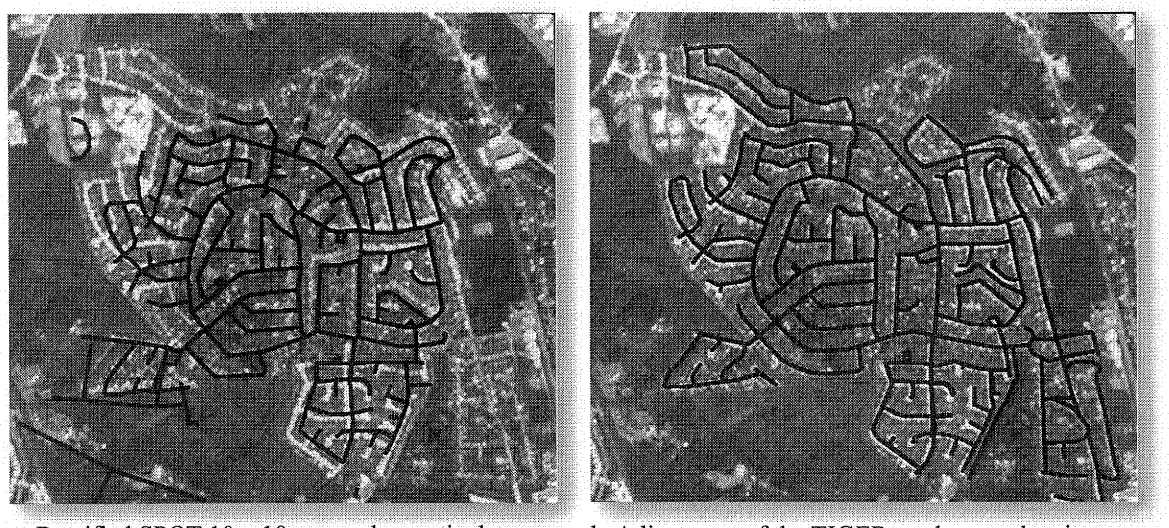

a. Rectified SPOT 10 x 10 m panchromatic data of an area near Irmo, SC, overlaid with the TIGER road network.

b. Adjustment of the TIGER road network using visual on-screen digitization.

Figure 12-21 a) U.S. Bureau of the Census TIGER road network data overlaid on SPOT 10 × 10 m panchromatic data of an area near Irmo, SC. b) Correction of the TIGER data based on visual on-screen movement of roads in error and digitization of entirely new roads.

Environmental experts agree that the current situation cannot be sustained. Yet, driven by poverty and their dependence upon exports, officials in the region have failed to take any preventive action, and the Aral Sea continues to shrink (NASA Aral Sea, 2004).

Atmospheric Correction for Change Detection

Now that many of the most widely adopted change detection algorithms have been identified, it is useful to provide some general guidelines about when it is necessary to atmospherically correct the individual dates of imagery used in the change detection process.

When Atmospheric Correction Is Necessary

Atmospheric correction of multiple-date remote sensor data is required when the individual date images used in the change detection algorithm are based on linear transformations of the data, e.g., a normalized difference vegetation index image is produced for Date 1 and Date 2. The additive effects of the atmosphere on each date contaminate the NDVI values and the modification is not linear (Song et al., 2001). Contributions from the atmosphere to NDVI values are significant and can amount to 50% or more over thin or broken vegetation cover (McDonald et al., 1998; Song et al., 2001). Similarly, the imagery should be atmospherically corrected if the change detection is based on multiple-date red/near-infrared ratioed images (e.g., Landsat TM 4/TM 3). This suggests that it may be necessary to normalize or atmospherically correct the multiple-date imagery used to compute the linearly transformed data (e.g., NDVI) when the goal is to identify *biophysical* change characteristics through time rather than just land-cover change through time (Yuan and Elvidge, 1998; Song et al., 2001; Du et al., 2002).

A change/no change map produced using image differencing logic and atmospherically corrected data normally looks different from a change/no change map produced using image differencing logic and non-atmospherically corrected data if the threshold boundaries are held constant in the change image histograms. However, if the analyst selects the appropriate thresholds in the two tails of the change detection image histogram, it doesn't really matter whether the change detection map was produced using atmospherically corrected or non-atmospherically corrected data. But, if the analyst desires that all stable classes in the change image have a value of 0 in the change histogram (refer to Figures 12-10

Impact of Hurricane Hugo Extracted Using Visual On-screen Change Detection

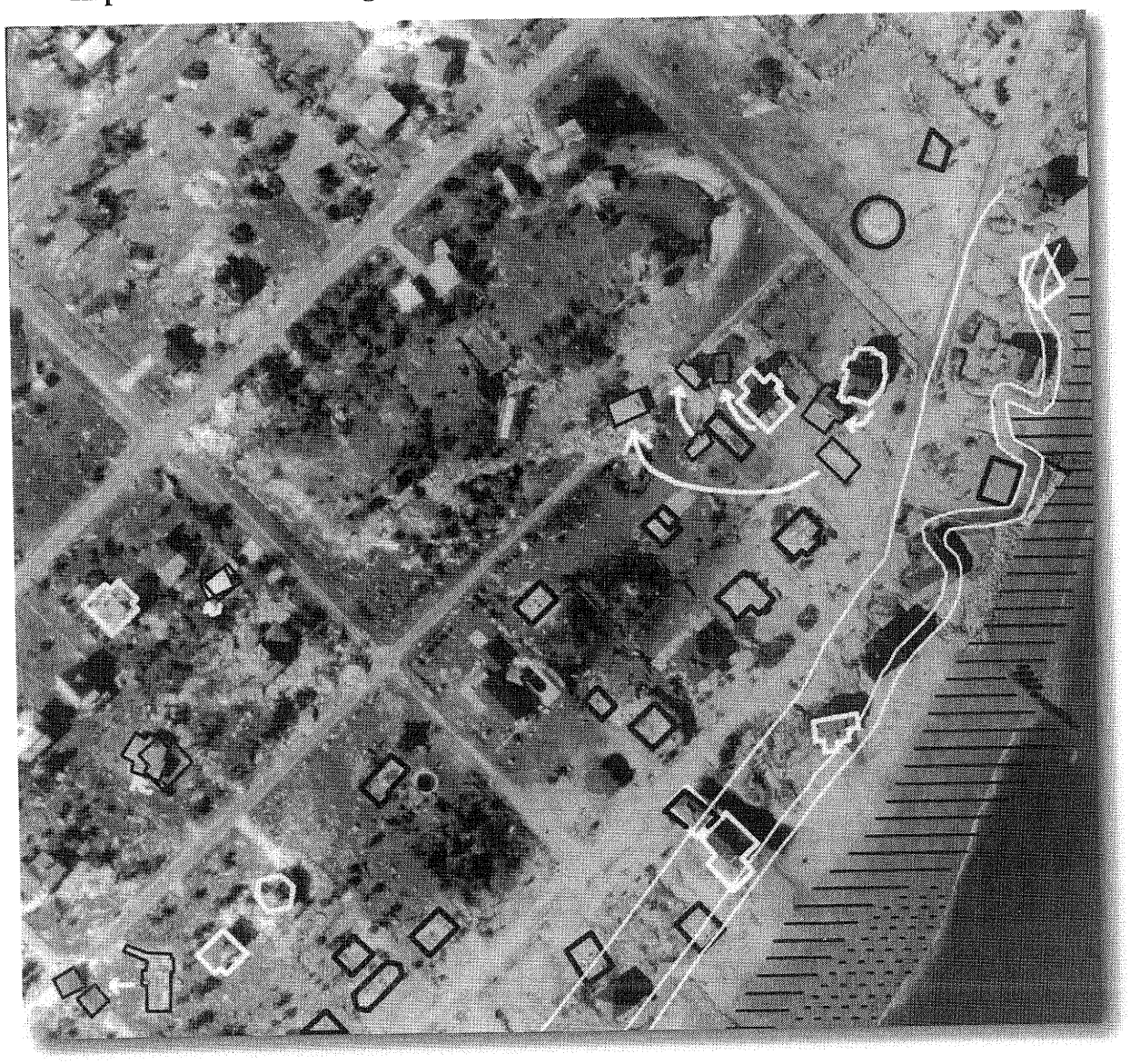

Figure 12-20 Change information overlaid on October 5, 1989, post-Hurricane Hugo aerial photograph, Sullivan's Island, SC. Completely destroyed houses are outlined in white. Partially destroyed houses are outlined in black. A white arrow indicates the direction of houses removed from their foundations. Three beachfront management setback lines are shown in white (base, 20 year, 40 year). Areas of beach erosion are depicted as black lines. Areas of beach accretion caused by Hurricane Hugo are shown as dashed black lines.

The shrinking Aral Sea has also had a noticeable effect on the region's climate. The growing season is now shorter, causing many farmers to switch from cotton to rice, which requires even more diverted water. A secondary effect of the reduction in the Aral Sea's overall size is the rapid exposure of the lake bed. Strong winds that blow across this part of Asia routinely pick up and deposit tens of thousands of tons of now-exposed soil every year. This process has caused a reduction in air quality for nearby residents and affected crop yields due to the heavily salt-laden particles falling on arable land.

and 12-11), then it is useful to normalize one image to another or atmospherically correct both images to percent reflectance values prior to performing image differencing.

Obtaining quality training data is very expensive and time-consuming because it usually involves people and field-work. Therefore, it will become increasingly important to be able to extend training data through both time and space. In other words, training data extracted from a Date 1 image should be able to be extended to a Date 2 image of the same geographic area (signature extension through time) or perhaps even to a Date 1 or Date 2 image of a neighboring geographic area (signature extension through space). Extending training data through space and time will require that each image evaluated be atmospherically corrected to surface reflectance whenever possible using one of the techniques described in Chapter 6. Nevertheless, it is not always necessary to correct remote sensor data when classifying individual dates of imagery or performing change detection.

When Atmospheric Correction Is Unnecessary

A number of studies have documented that it is unnecessary to correct for atmospheric effects prior to image classification if the spectral signatures characterizing the desired classes are derived from the image to be classified (e.g., Kawata et al., 1990). This is because atmospherically correcting a single date of imagery is often equivalent to subtracting a constant from all pixels in a spectral band. This action simply translates the origins in multidimensional feature space. The class means may change, but the variance–covariance matrix remains the same irrespective of atmospheric correction. In other words, atmospheric correction is unnecessary as long as the training data and the data to be classified are in the same relative scale (corrected or uncorrected) (Song et al., 2001). This suggests that it is not necessary to atmospherically correct Landsat TM data obtained on Date 1 if it is going to be subjected to a maximum likelihood classification algorithm and all the training data are derived from the Date 1 imagery. The same holds true when a Date 2 image is classified using training data extracted from the Date 2 image. Change between the Date 1 and Date 2 classification maps derived from the individual dates of imagery (corrected or uncorrected) can easily be compared in a post-classification comparison.

Atmospheric correction is also unnecessary when change detection is based on classification of multiple-date composite imagery in which the multiple dates of remotely sensed images are rectified and placed in a single dataset and then classified as if it were a single image (e.g., multiple-date principal components change detection). Only when training data from one time and/or place are applied in another time and/or place is atmospheric correction necessary for image classification and many change detection algorithms.

Summary

A one-time inventory of natural resources is often of limited value. A time series of images and the detection of change provides significant information on *the resources at risk* and may be used in certain instances to identify *the agents of change*. Change information is becoming increasingly important in local, regional, and global environmental monitoring (Woodcock et al., 2001). This chapter identifies the remote sensor system and environmental variables that should be considered whenever a remote sensing change detection project is initiated. Several useful change detection algorithms are reviewed. Scientists are encouraged to carefully review and understand these principles so that accurate change detection can take place.

References

Arzandeh, S. and J. Wang, 2003, "Monitoring the Change of Phragmites Distribution Using Satellite Data," *Canadian Journal of Remote Sensing*, 29(1):24–35.

Bauer, M. E., Burk, T. E., Ek, A. R., Coppin, P. R., Lime, S. D., Walsh, T. A., Walters, D. K., Befort, W. and D. F. Heinzen, 1994, "Satellite Inventory of Minnesota Forest Resources," *Photogrammetric Engineering & Remote Sensing* 60(3):287–298.

Chen, J., Gong, P., He, C., Pu, R. and P. Shi, 2003, "Land-Use/Land-Cover Change Detection Using Improved Change-Vector Analysis," *Photogrammetric Engineering & Remote Sensing* 69(4):369–379.

Civco, D. L., 1989, "Topographic Normalization of Landsat Thematic Mapper Digital Imagery," *Photogrammetric Engineering & Remote Sensing*, 55(9):1303–1309.

Civco, D. L., Hurd, J. D., Wilson, E. H., Song, M. and Z. Zhang, 2002, "A Comparison of Land Use and Land Cover Change Detection Methods," *Proceedings*, *ASPRS-ACSM Annual Conference and FIG XXII Congress,* Bethesda, MD: American Society for Photogrammetry & Remote Sensing, 10 p, CD.

Collins, J. B. and C. E. Woodcock, 1996, "An Assessment of Several Linear Change Detection Techniques for Mapping Forest Mortality Using Multitemporal Landsat TM Data," *Remote Sensing of Environment*, 56:66–77.

Cowen, D. J., J. R. Jensen, and J. Halls, 1991, "Maintenance of TIGER Files Using Remotely Sensed Data," *Proceedings*, *American Society for Photogrammetry & Remote Sensing*, (4):31–40.

Dobson, J. E., Ferguson, R. L., Field, D. W., Wood, L. L., Haddad, K. D., Iredale, H., Jensen, J. R., Klemas, V. V., Orth, R. J. and J. P. Thomas, 1995, *NOAA Coastal Change Analysis Project (C-CAP): Guidance for Regional Implementation,* Washington: NOAA, NMFS 123, 92 p.

Du, Y., Teillet, P. M. and J. Cihlar, 2002, "Radiometric Normalization of Multitemporal High-resolution Satellite Images with Quality Control for Land Cover Change Detection," *Remote Sensing of Environment*, 82:123–134.

Eastman, J. R. and M. Fulk, 1993, "Long Sequence Time Series Evaluation Using Standardized Principal Components," *Photogrammetric Engineering & Remote Sensing*, 59(6):991–996.

Eckhardt, D. W., Verdin, J. P. and G. R. Lyford, 1990, "Automated Update of Irrigated Lands GIS Using SPOT HRV Imagery," *Photogrammetric Engineering & Remote Sensing*, 56(11):1515–1522.

Foody, G. M., 2001, "Monitoring the Magnitude of Land-Cover Change Around the Southern Limits of the Sahara," *Photogrammetric Engineering & Remote Sensing*, 67(7):841–847.

Franklin, S. E., Lavigne, M. B., Wulder, M. A. and T. M. McCaffrey, 2002, "Large-area Forest Structure Change Detection: An Example," *Canadian Journal of Remote Sensing*, 28(4):588–592.

Fung, T. and E. LeDrew, 1988, "The Determination of Optimal Threshold Levels for Change Detection Using Various Accuracy Indices," *Photogrammetric Engineering & Remote Sensing,* 54(10):1449–1454.

Green, K., Kempka, D. and L. Lackey, 1994, "Using Remote Sensing to Detect and Monitor Land-cover and Land-use Change," *Photogrammetric Engineering & Remote Sensing* 60(3):331–337.

Gong, P., LeDrew, E. F. and J. R. Miller, 1992, "Registration-noise Reduction in Difference Images for Change Detection," *International Journal of Remote Sensing,* 13(4):773–779.

Jensen, J. R., 1981, "Urban Change Detection Mapping Using Landsat Digital Data," *The American Cartographer*, 8(2):127–147.

Jensen, J. R., 2000, *Remote Sensing of the Environment: An Earth Resource Perspective*, Upper Saddle River, NJ: Prentice-Hall, 544 p.

Jensen, J. R., Botchway, K., Brennan-Galvin, E., Johannsen, C., Juma, C., Mabogunje, A., Miller, R., Price, K., Reining, P., Skole, D., Stancioff, A. and D. R. F. Taylor, 2002, *Down to Earth: Geographic Information for Sustainable Development in Africa*, Washington: National Research Council, 155 p.

Jensen, J. R., Cowen, D. J., Narumalani, S., Althausen, J. D. and O. Weatherbee, 1993a, "An Evaluation of CoastWatch Change Detection Protocol in South Carolina," *Photogrammetric Engineering & Remote Sensing*, 59(6):1039–1046.

Jensen, J. R., Huang, X. and H. E. Mackey, 1997, "Remote Sensing of Successional Changes in Wetland Vegetation as Monitored During a Four-Year Drawdown of a Former Cooling Lake," *Applied Geographic Studies*, 1:31–44.

Jensen, J. R., S. Narumalani, O. Weatherbee and H. E. Mackey, 1993b, "Measurement of Seasonal and Yearly Cattail and Waterlily Changes Using Multidate SPOT Panchromatic Data," *Photogrammetric Engineering & Remote Sensing*, 59(4):519–525.

Jensen, J. R., Rutchey, K., Koch, M. and S. Narumalani, 1995, "Inland Wetland Change Detection in the Everglades Water Conservation Area 2A Using a Time Series of Normalized Remotely Sensed Data," *Photogrammetric Engineering & Remote Sensing*, 61(2):199–209.

Kawata, Y., Ohtani, A., Kusaka, T. and S. Ueno, 1990, "Classification Accuracy for the MOS-1 MESSR Data Before and After the Atmospheric Correction," *IEEE Transactions Geoscience Remote Sensing*, 35:1–13.

Kim, H. H. and G. C. Elman, 1990, "Normalization of Satellite Imagery," *International Journal of Remote Sensing*, 11(8):1331–1347.

Koeln, G. and J. Bissonnette, 2000, "Cross-correlation Analysis: Mapping Land Cover Change with a Historic Land Cover Database and a Recent, Single-date Multispectral Image," *Proceedings*, *American Society for Photogrammetry & Remote Sensing,* Bethesda, MD: ASPRS, 8 p., CD.

Light, D., 1993, "The National Aerial Photography Program as a Geographic Information System Resource," *Photogrammetric Engineering & Remote Sensing*, 59(1):61–65.

Lyon, J. G., Yuan, D., Lunetta, R. S. and C. D. Elvidge, 1998, "A Change Detection Experiment Using Vegetation Indices," *Photogrammetric Engineering & Remote Sensing*, 64:143–150.

Lunetta, R. S. and C. Elvidge, 2000, *Remote Sensing Change Detection: Environmental Monitoring Methods and Applications*, New York: Taylor & Francis, 340 p.

Lunetta, R. L. and J. G. Lyons (Eds.), 2003, *Geospatial Data Accuracy Assessment,* Las Vegas: US Environmental Protection Agency, Report No. EPA/600/R-03/064, 335 p.

Lunetta, R. S., Congalton, R. G., Fenstermaker, L. K., Jensen, J. R., McGwire, K. C. and L. R. Tinney, 1991, "Remote Sensing and Geographic Information System Data Integration: Error Sources and Research Issues," *Photogrammetric Engineering & Remote Sensing,* 57(6):677–687.

Maas, J. F., 1999, "Monitoring Land-cover Changes: A Comparison of Change Detection Techniques," *International Journal of Remote Sensing*, 20(1):139–152.

Malila, W. A., 1980, "Change Vector Analysis: An Approach for Detecting Forest Changes with Landsat," *Proceedings, LARS Machine Processing of Remotely Sensed Data Symposium,* W. Lafayette, IN: Laboratory for the Applications of Remote Sensing, pp. 326–336.

McDonald, A. J., Gemmell, F. M. and P. E. Lewis, 1998, "Investigation of the Utility of Spectral Vegetation Indices for Determining Information on Coniferous Forests," *Remote Sensing of Environment*, 66:250–272.

Michalek, J. L., Wagner, T. W., Luczkovich, J. J. and R. W. Stoffle, 1993, "Multispectral Change Vector Analysis for Monitoring Coastal Marine Environments," *Photogrammetric Engineering & Remote Sensing*, 59(3):381–384.

NASA Aral Sea, 2004, *The Shrinking Aral Sea*, Washington: NASA Earth Observatory, http://earthobservatory.nasa.gov/Newsroom/NewImages/images.php3?img_id=4819.

Ridd, M. K. and J. Liu, 1998, "A Comparison of Four Algorithms for Change Detection in an Urban Environment," *Remote Sensing of Environment*, 63:95–100.

Rutchey, K. and L. Velcheck, 1994, "Development of an Everglades Vegetation Map Using a SPOT Image and the Global Positioning System," *Photogrammetric Engineering & Remote Sensing*, 60(6):767–775.

Skole, D., 1994, "Data on Global Land-cover Change: Acquisition, Assessment and Analysis," in W. B. Meyer and B. L. Turner, (Eds.), *Changes in Land Use and Land Cover: A Global Perspective,* Cambridge: Cambridge University Press, 437–471.

Song, C., Woodcock, C. E., Seto, K. C., Lenney, M. P. and S. A. Macomber, 2001, "Classification and Change Detection Using Landsat TM Data: When and How to Correct Atmospheric Effects," *Remote Sensing of Environment*, 75:230–244.

Virag, L. A. and J. E. Colwell, 1987, "An Improved Procedure for Analysis of Change in Thematic Mapper Image-Pairs," *Proceedings of the 21st International Symposium on Remote Sensing of Environment*, Ann Arbor: Environmental Research Institute of Michigan, 1101–1110.

Wang, F., 1993, "A Knowledge-based Vision System for Detecting Land Changes at Urban Fringes," *IEEE Transactions on Geoscience & Remote Sensing*, 31:136–145.

Woodcock, C. E., Macomber, S. A., Pax-Lenney, M. and W. B. Cohen, 2001, "Monitoring Large Areas for Forest Change Using Landsat: Generalization Across Space, Time and Landsat Sensors," *Remote Sensing of Environment*, 78:194–203.

Yuan, D. and C. Elvidge, 1998, "NALC Land Cover Change Detection Pilot Study: Washington D.C. Area Experiments," *Remote Sensing of Environment*, 66:166–178.

Zhan, X., Sohlberg, R. A., Townshend, J. R. G., DiMiceli, C., Carroll, M. L., Eastman, J. C., Hansen, M. C. and R. S. DeFries, 2002, "Detection of Land Cover Changes Using MODIS 250 m Data," *Remote Sensing of Environment*, 83:336–350.

Thematic Map Accuracy Assessment 13

Information derived from remotely sensed data are becoming increasingly important for environmental models at local, regional, and global scales (Johannsen et al., 2003). The remote sensing–derived thematic information may be in the form of thematic maps or statistics derived from area-frame sampling techniques. The thematic information must be accurate because important decisions are made throughout the world using the information (Muchoney and Strahler, 2002; Kyriakidis et al., 2003).

Unfortunately, the thematic information contains error. Scientists who create remote sensing–derived thematic information should recognize the sources of the error, minimize it as much as possible, and inform the user how much confidence he or she should have in the thematic information. Remote sensing–derived thematic maps should normally be subjected to a thorough accuracy assessment before being used in scientific investigations and policy decisions (Stehman and Czaplewski, 1998; Paine and Kiser, 2003).

Land-use and Land-cover Map Accuracy Assessment

The steps generally taken to assess the accuracy of thematic information derived from remotely sensed data are summarized in Figure 13-1. First, it is important to clearly state the nature of the thematic accuracy assessment problem at hand, including:

- what the accuracy assessment is expected to accomplish,
- the classes of interest (discrete or continuous), and
- the sampling design and sampling frame (consisting of area and list frames).

The objectives of the accuracy assessment should be clearly identified. Sometimes a simple qualitative examination may be appropriate if the remote sensing–derived data are to be used as general undocumented information. Conversely, if the remote sensing–derived thematic information will impact the lives of human beings, flora, fauna, etc., then it may be necessary to conduct a thorough probability design-based accuracy assessment.

The accuracy assessment sampling design is the protocol (i.e., instructions) by which the reference sample units are selected (Stehman and Czaplewski, 1998). Sampling designs generally require a *sampling frame* that consists of